Cross-species metabolomic analysis of DDT and Alzheimer's disease-associated tau toxicity

Vrinda Kalia[1], Megan M. Niedzwiecki[2], Joshua M. Bradner[1], Fion K. Lau[1], Meghan L. Bucher[1], Katherine E. Manz[3], Zoe Coates Fuentes[2], Kurt D. Pennell[3], Martin Picard[4], Douglas I. Walker[2], William T. Hu[5], Dean P. Jones[6], Gary W. Miller[1]

[1] Department of Environmental Health Sciences, Mailman School of Public Health, Columbia University, New York, NY, USA

[2] Department of Environmental Medicine and Public Health, Icahn School of Medicine at Mount Sinai, New York, NY, USA

[3] School of Engineering, Brown University, Providence, RI, USA

[4] Department of Neurology, Department of Psychiatry, Columbia University Irving Medical Center, New York, NY, USA

[5] Department of Neurology, Rutgers Biomedical and Health Sciences, New Brunswick, NJ, USA

[6] Division of Pulmonary, Allergy and Critical Medicine, Department of Medicine, School of Medicine, Emory University, Atlanta, GA, USA

Corresponding authors:

Gary W. Miller: gm2815@columbia.edu or Vrinda Kalia: vk2316@columbia.edu

722 W 168th street, New York, NY 10032

Abstract

Background. The formation of hyperphosphorylated tau (p-tau) protein tangles in neurons is a pathological marker of Alzheimer's disease (AD). Exposure to the pesticide dichlorodiphenyltrichloroethane (DDT) has been associated with increased risk of AD.

Objectives. To determine if there was a connection between DDT exposure and tau toxicity we investigated whether exposure to DDT can exacerbate tau protein toxicity in *C. elegans.* In addition, we examined the association between p-tau protein and metabolism in a human population study and in a transgenic *C. elegans* strain neuronally expressing a mutant tau protein fragment that is prone to aggregation.

Methods. In the human population study, we used a metabolome-wide association framework to determine the association between p-tau measured in the cerebrospinal fluid (CSF) and metabolomic features measured in both plasma (n = 142) and CSF (n = 78) using high-resolution metabolomics (HRM). Using the same HRM method, we determined changes in metabolomic features in the transgenic *C. elegans* strain compared to its control strain. Metabolites associated with p-tau in both species were analyzed for overlap. We also examined the effect of DDT and aggregating tau protein on growth, swim behavior, mitochondrial function, metabolism, learning, and lifespan in *C. elegans*.

Results. Plasma and CSF-derived features associated with p-tau level were related to drug, amino acid, fatty acid and mitochondrial metabolism pathways. Five metabolites overlapped between plasma and *C. elegans*, and 4 between CSF and *C. elegans*. DDT exacerbated the inhibitory effect of aggregating tau protein on growth and basal respiration. In the presence of aggregating tau protein, DDT induced more curling and

was associated with reduced levels of amino acids but increased levels of uric acid and adenosylselenohomocysteine. Developmental exposure to DDT blunted the lifespan reduction caused by aggregating tau protein.

Conclusion. The model organism *C. elegans* can complement human studies by providing a means to study mechanisms of environmental toxicants. Specifically, our *C. elegans* data show that DDT exposure and tau protein aggregation both inhibit mitochondrial function and DDT exposure can exacerbate the mitochondrial inhibitory effects of tau protein aggregation providing a plausible explanation for the observed human associations.

Main text

Introduction

In 2014, 5 million people in the US were living with Alzheimer's disease (AD). By 2060, this number is projected to grow to 13.9 million (Matthews et al. 2019). Clinically, AD manifests as dementia, a progressive deterioration of memory and cognitive function (Van Cauwenberghe et al. 2016). Pathologically, AD is characterized by severe neuronal loss, aggregation of amyloid-β (Aβ) in extracellular senile plaques, and formation of intraneuronal neurofibrillary tangles consisting of hyperphosphorylated tau (p-tau) protein. There is evidence that AD may be a metabolic neurodegenerative disease (de la Monte and Wands 2008) as it has been associated with altered local and peripheral metabolism in several studies. Through *in vitro*, animal model, and epidemiological studies, investigators have found associations between tau neurofibrillary tangles and impaired glucose metabolism (Bischof and Park 2015; Ossenkoppele et al. 2015, 2016), altered mitochondrial trafficking, morphology and bioenergetics, and reduced ATP production (Pérez et al. 2018). While aging is the strongest risk factor of AD, evidence of risk factors for dementias show that lifestyle choices and the environment may modify disease onset and alter the projected prevalence (Nichols et al. 2019). Indeed, using untargeted high-resolution metabolomics (HRM), our group has uncovered plasma derived metabolites from endogenous and exogenous sources associated with the disease (Niedzwiecki et al. 2020; Vardarajan et al. 2020). If causally associated with the disease, these metabolites may be modified or targeted to alter disease prevalence or progression.

The role of the environment in AD pathogenesis has a controversial history (DeKosky and Gandy 2014) but recent studies provide evidence of environmental chemical exposures influencing disease risk. In a cross-sectional, case-control study, Richardson and colleagues found that cases of AD had higher levels of a metabolite of the pesticide DDT (1,1,1-tricholoro-2,2-bis(p-chloro-phenyl) ethane) in their serum (Richardson et al. 2014). DDT is a highly persistent, synthetic organochlorine pesticide used for pest control in agricultural settings and to control vectors that can cause diseases like malaria and typhus. It was widely used in the USA from 1939 to 1972, until its use was banned by the US Environmental Protection Agency (EPA) (Turusov et al. 2002). Despite its regulation, DDT and its metabolites remain persistent and can be detected in the blood of most of the US population (National Report on Human Exposure to Environmental Chemicals | CDC 2020). Additionally, DDT can be passed through breastmilk to infants, exposing generations that have been born after its ban (Needham et al. 2011). DDT is still used for vector control in some African and south Asian countries (van den Berg et al. 2017) and can travel long distances through evaporation, distillation, and transport via winds and ocean currents (Wania and Mackay 1996). Therefore, DDT poses a threat to the health of populations living in countries where it is still produced and in countries that are further away.

Caenorhabtidis elegans (*C. elegans* or worms) is a non-parasitic nematode that has long been used in neuroscience and developmental research; more recently it has been gaining popularity as an *in vitro* model in toxicity testing. Studies in *C. elegans* show that the toxicity ranking of several toxicants, including, but not limited to, metals, organophosphate pesticides, ~ 60% of chemicals in the EPA's ToxCast^{TM} Phase I and

Phase II libraries, known or suspected developmental toxicants, and metabolic toxicants, is predictive of rat LD_{50} values (Boyd et al. 2016; Cole et al. 2004; Harlow et al. 2016; Hunt 2017; Hunt et al. 2012; Middendorf and Dusenbery 1993; Williams and Dusenbery 1988). The model is inexpensive and requires minimal laboratory expertise to maintain. Several fundamental aspects of biology were discovered in *C. elegans* including apoptosis, RNAi, and miRNA. Furthermore, *C. elegans* are the first complex organism to have their genome sequenced (*C. elegans* Sequencing Consortium 1998), allowing access to a large library of genetic mutant strains. The long history of its use in biology and the conservation of several genes and pathways between worms and humans (Kaletta and Hengartner 2006) makes the nematode model valuable for biological insight (Brenner 1974; Corsi et al. 2015), particularly to study gene-environment interactions.

In this study, we use untargeted liquid chromatography (LC) with high-resolution mass spectrometry to identify plasma and cerebrospinal fluid (CSF) derived metabolites associated with p-tau levels measured in the CSF of individuals from a clinical study of AD. We then compared metabolites associated with p-tau to the metabolic profile of a transgenic strain of *C. elegans* that is a model of AD-related pathology which expresses a mutant fragment of tau protein in all neurons (Fatouros et al. 2012). Using the same mutant tau transgenic strain of *C. elegans* (Fatouros et al. 2012), we then tested the effect of exposure to DDT on growth, behavior, metabolism, learning, and survival.

Methods

1. Chemicals. BD Bacto dehydrated agar, salts to make M9 buffer (monobasic potassium phosphate, dibasic sodium phosphate, sodium chloride, magnesium sulfate), 1N sodium

hydroxide, p,p'-DDT (>95%), dimethyl sulfoxide (DMSO, 99.9%), acetone (99.8%, HPLC grade), n-hexane (>=99%), dichloromethane (99.8%, HPLC grade), sodium azide (99%), and 2-butanone (≥ 99.0%) were purchased from Fisher Scientific (Waltham, MA). Carbonyl cyanide 4-(trifluoromethoxy) phenylhydrazone (FCCP, > 98%) was purchased from Sigma-Aldrich (St. Louis, MO). Certified reference standards for GC-HRMS quantification were purchased from Accustandard (New Haven, CT), including o,p'-DDT, p,p'-DDT, o,p'-DDE, p,p'-DDE, $^{13}C_{12}$ labeled p,p'-DDE, D_8 labeled p,p'-DDT, phenanthrene D-10, and chrysene D-12. The hypochlorite solution used for synchronization was prepared using household bleach (Clorox, 8% sodium hypochlorite), water, and 1N sodium hydroxide.

2. Human: participants and sample collection. This study was approved by the Emory University Institutional Review Board and the methods have been previously described (Niedzwiecki et al. 2020). Briefly, subjects were recruited from the Emory Cognitive Neurology Clinic and the Emory Alzheimer's Disease Research Center. Each subject underwent a detailed neurological and neuropsychological evaluation. Subjects were classified as having normal cognition (NC) if there was no subjective cognitive complaint and neuropsychological analysis showed normal cognitive functioning for their age, gender, education, and race; mild cognitive impairment (MCI) (Albert et al. 2011), or AD dementia (McKhann et al. 2011) according to NIA-AA criteria (Niedzwiecki et al. 2020). Plasma and CSF samples were collected and processed as described previously (Hu et al. 2015; Niedzwiecki et al. 2020). CSF AD biomarker analysis was performed as

previously described using a Luminex 200 platform to determine levels of total tau (t-Tau), and tau phosphorylated at threonine 181 (p-Tau_{181}) (Howell et al. 2017).

3. *C. elegans* methods

3.1. *C. elegans*: growth and maintenance. Standard methods of culture, including the use of normal or high growth media (NGM/HGM) plates, culture temperature of 20 °C and the OP50 *E. coli* strain as a food source, were followed as described (Brenner 1974) unless noted otherwise. *C. elegans* strains used included the wild type N2 Bristol strain, BR5271 (*byIs162* [P_{rab-3}::F3(delta)K280 I277P I380P + P_{myo-2}::mCherry]; referred to as the "non-aggregating/non-agg" strain), and BR5270 (*byIs161* [P_{rab-3}::F3(delta)K280 + P_{myo-2}::mCherry]; referred to as the "aggregating/agg" strain). All strains were provided by the Caenorhabditis Genetics Center, which is funded by NIH Office of Research Infrastructure Programs (P40 OD010440).

3.2. *C. elegans*: exposure to DDT. Worms were exposed to the pesticide p,p'-DDT or the solvent control, DMSO, on NGM plates. DDT exposure plates were created using methods previously described (Hunt et al. 2011). Briefly, a 20 mM stock of DDT, made by dissolving in 100% DMSO, was diluted to 150 μM with sterile water and then applied on the surface of NGM plates spotted with OP50 *E. coli* to obtain the appropriate final concentration of DDT on the plate. The solvent control plates were created following the same dilution but without DDT to achieve a final concentration of 0.015% DMSO. DDT was allowed to diffuse and the plates were allowed to equilibrate for 2 hours before worms

were introduced. All worms were exposed to a final concentration of 3 μM DDT unless otherwise stated.

3.3. *C. elegans*: DDT uptake experiments. A synchronized population of wildtype worms, created using hypochlorite treatment, were grown on 10 cm NGM plates with 0.3, 3, or 30 μM DDT, and the DMSO control. The non-aggregating and aggregating worms were similarly synchronized and exposed to 3 μM DDT or DMSO. All strains were collected after 72 hours of exposure, at the young adult stage. They were washed in M9 buffer 4x and sorted into aliquots of 1000-1200 worms using the COPAS FP-250. The volume of M9 buffer in each sample was reduced to 100 μL and each sample was snap frozen in liquid nitrogen. To extract DDT and its metabolites, the worm cuticle was disrupted by bead beating (6.5 m/s for 1 minute) and the samples were analyzed for levels of DDT.

3.4. *C. elegans*: growth determined through size measured on COPAS Biosorter. The COPAS Flow Pilot (FP) 250 is an instrument used for high-throughput manipulation of *C. elegans*. For each worm that passes through the flow cell, the COPAS FP-250 determines its time-of-flight (TOF), which represents the length of the worm passing through the flow cell, and the extinction, which represents the optical density or thickness of the worm passing through the flow cell. After hypochlorite synchronization, eggs from all three strains were allowed to hatch and develop on 10 cm NGM plates with 3 μM DDT or DMSO. Worms were sorted through the COPAS FP 250 to measure TOF and extinction 46-50 hours after synchronization (around the L4 stage, n = 1000-4000 per

group, object inclusion criteria: Log(TOF) > 6 and Log(extinction) > 5) and at 70-72 hours post synchronization (young adults, *n* = 1000-4000 per group, object inclusion criteria: Log(extinction) between 5.5 and 9). We used inclusion criteria that have been previously estimated for the L4 larval and adult stage on the COPAS FP-250 (Boyd et al. 2016). Measures of TOF and extinction were compared across the strains and treatment groups using a one-way analysis of variance at the two time points.

3.5. *C. elegans*: swim behavior. The celeST software package was used to determine aspects of swim behavior for the different strains exposed to DDT or the solvent control (Restif et al. 2014). Briefly, 3-4 worms at the young adult stage were placed in 60 μL of M9 buffer in a 15 mm ring preprinted on a microscope slide (Fisherbrand microscope slides with two 15 mm diameter circles, catalog #22-339-408). Recordings of swim behavior were made as a series of jpeg images using a chameleon 3 camera (FLIR, Wilsonville, OR) for 30 s at a frame rate of 18 f/s. Data were collected from four-five trials representing different experiments, with a total of 50-100 worms recorded per group.

3.6. *C. elegans*: seahorse XFe96 extracellular flux analysis. The three strains exposed to DDT or solvent control were collected at the young adult stage and washed in M9 buffer 4x for analysis using the Seahorse XFe96 extracellular flux analyzer (Koopman et al. 2016). Briefly, 3-30 worms in M9 buffer were plated into the wells of a Seahorse utility plate and the volume of M9 buffer in each well was made up to 200 μL. M9 buffer without any worms was used as the blank for background correction. Baseline respiration was measured (measurement numbers 1-5), followed by injection of FCCP (10 μM, final

concentration) to elicit maximal respiration (measurement number 6-14), followed by sodium azide (40 mM, final concentration) to measure non-mitochondrial respiration (measurement number 15-18). Data were normalized to the number of worms in each well to determine the rate of oxygen consumption (pmol O_2/min) per worm. Basal respiration was determined as the difference between non-mitochondrial respiration and the average oxygen consumption rate at measurements 2 through 5; maximal respiration was determined as the difference between non-mitochondrial respiration and the average oxygen consumption rate measured after the FCCP injection; and spare respiratory capacity was measured as the difference between basal and maximal respiration.

3.7. *C. elegans*: associative learning assay. The associative learning assay was carried out as previously described (Kauffman et al. 2011) with some modifications. The assay relies on an associative memory paradigm where worms are trained by pairing the presence of food with the odor of 10% butanone. Briefly, worms were hypochlorite synced and allowed to grow on DDT or solvent control plates for about 72 hours, until they reached the young adult stage. Worms were collected off plates and washed 3x in M9 buffer. After the last wash, the naïve attraction toward butanone was assessed. Worms were then starved for an hour, after which the conditioned training was performed to pair the odor with the presence of food. The attraction toward butanone was determined just after conditioning, representing their ability to learn and form an associative memory. To count the number of worms attracted to the butanone spot or the control (95% ethanol) spot, images of the entire assay plates were taken on a Basler GigE camera, and the

images were analyzed using a MATLAB algorithm created by the Murphy lab (Kauffman et al. 2011).

3.8. *C. elegans*: survival analysis. Wildtype worms and the transgenic strains were exposed to DDT or DMSO until the young adult stage, around 72 hours. After exposure, worms were collected off plates and washed in M9 buffer 4 times. We created 4 replicates per treatment group per strain with 25-35 worms each. Adult worms were counted and transferred everyday onto new 6 cm NGM plates until they stopped producing progeny (~ adult day 6). At this point, worms were transferred onto 6 cm NGM plates with nystatin and ampicillin. Worms were then counted every other day and scored as dead if they did not respond to the gentle touch of a platinum wire. A worm was censored from the plate if it was missing, showed internal hatching, or was damaged during transfer. Worms were followed until they were all dead. Data was analyzed using Kaplan Meier survival calculations and the log-rank test using the R package survival.

4. High-resolution mass spectrometry methods.

4.1. Gas chromatography with high- resolution mass spectrometry (GC-HRMS) for *C.* elegans DDT uptake. Worm tissue concentrations of p,p'-DDT, p,p'-DDE, p,p'-DDD, o,p'-DDT, o,p'-DDE and o,p'-DDD were measured using methods previously described (Elmore et al. 2020). Prior to extraction, each sample was spiked with labeled isotope internal standards to assess analyte recovery. Each sample was extracted using QuEChERS (Quick, Easy, Cheap, Effective, Rugged, Safe). The samples were first vortex mixed in centrifuge tubes with 1 mL 1:1:1 hexane:acetone:dichloromethane and

sonicated for 30 minutes. The entire sample and the supernatant were transferred to a centrifuge tube containing 150 g MgSO4 and 50 mg C18 (United Chemical Technologies, Bristol, PA), vortexed for 30 seconds, and centrifuged for 5 minutes at 1,105 x g. This extraction was repeated 2 more times and the final 3 mL extract was evaporated to 150 μL under nitrogen (Organomation 30 position Multivap Nitrogen Evaporator), transferred to a low-volume (300 μL) GC vial, and spiked with phenanthrene-D10 and chrysene-D12 as volumetric internal standards to ensure injection consistency during GC-HRMS analysis. Extracts were analyzed on a GC Q-Exactive Orbitrap MS (Thermo Scientific) equipped with a Thermo Trace 1300 gas chromatograph and TriPlus RSH Autosampler using chromatographic methods described previously (Elmore et al. 2020). The MS was operated in full scan mode, with a scan range of 50 to 750 m/z. Analytes were quantified using the most abundant fragment and identity was confirmed using the ratio of two confirming ions and retention times (Supplemental Table 1).

4.2. Sample preparation for liquid chromatography coupled high resolution mass spectrometry (LC-HRMS).

Human sample preparation: Samples were prepared for HRM using methods detailed elsewhere (Go et al. 2015; Niedzwiecki et al. 2020; Park et al. 2012; Soltow et al. 2013). Briefly, aliquots of plasma or CSF were removed from -80 °C storage and thawed on ice. 65 μL of each biofluid was added to 130 μL of acetonitrile containing a mixture of stable isotopic standards, vortexed, and allowed to equilibrate for 30 min. Proteins were precipitated by centrifuge (16,100 x g at 4 °C for 10 min) and the supernatant was transferred to a low-volume vial for analysis.

C. elegans sample preparation: two different experiments were conducted and prepared: 1. To determine the metabolic effects of aggregating tau protein, a synchronized population of worm eggs of the non-aggregating and aggregating strain were allowed to hatch and grow on NGM plates. 2. To determine the effect of DDT on metabolism in all strains, a synchronized population of all strains, wildtype, non-aggregating and aggregating worms, were placed on NGM plates coated with DDT or DMSO. In both experiments, worms were allowed to grow until larval stage 4. For collection, worms were washed 4x in M9 buffer and sorted into four-to-six replicates containing 500 worms using a COPAS FP-250. The final volume was reduced to 100 μL by centrifuge and each sample was snap frozen in liquid nitrogen and stored at -80 °C until needed for processing. Metabolites were extracted using methods described previously (Bradner et al. 2021; Mor et al. 2020). Briefly, two volumes of acetonitrile (200 μL) containing a mixture of internal standards was added to the 100μL worm suspension, and samples were homogenized by bead-beating. A spatula-full of zirconium oxide beads (~10 beads, 0.5 mm diameter, Yttria stabilized) from Next Advance (Troy, NY) was added to each worm sample, and placed in a bead beater (Next Advance Bullet Blender Storm, Troy, NY) set at 6.5 m/s for 30 seconds. Extracts were then allowed to equilibrate on ice for one minute, and placed in the beater for another 30 seconds at the same speed. After equilibration on ice for 30 minutes, proteins were removed by centrifuge (15,000 x g at 4 °C for 10 min). All sample processing was performed on ice or in a cold room when necessary.

4.3. High-resolution metabolomic analyses. Human sample extracts were analyzed by reverse-phase C18 liquid chromatography (Dionex Ultimate 3000) and Fourier transform mass spectrometry in positive electrospray ionization mode, resolution (FWHM) of 70,000 (Niedzwiecki et al. 2020). Sample extracts from *C. elegans* were analyzed on an LC-HRMS platform in two ways: 1. For determination of the effect of aggregating tau protein on metabolism, sample extracts were analyzed using untargeted LC-HRMS using methods described previously (Liu et al. 2020). Mass spectral data were generated under positive electron spray ionization in full scan mode. 2. Due to changes in LC-HRMS technologies, analysis of DDT exposure studies used slightly different analytical conditions; however, detection of endogenous metabolites across the two platforms is consistent. For determination of the effect of DDT on metabolism in all strains, after processing, the supernatant was diluted 1:1 in HPLC-grade water and analyzed using a HILIC column (positive and negative ESI mode) and C18 column (positive and negative ESI mode). Separation was similar to conditions described above, except an acetonitrile gradient with 10 mM ammonium acetate was used for HILIC, and acetonitrile gradient with 0.5% acetic acid for C_{18}. For both methods, 10 μL of the sample extract was injected in triplicate. All mass spectral data were generated on an orbitrap mass spectrometer in full scan mode (1: Thermo Scientific Q-Exactive HF and 2: Thermo Scientific HFX), scanning for mass range 85 to 1250 Da. All raw mass spectral data were extracted using the R packages apLCMS (Yu et al. 2009) and xMSanalyzer (Uppal et al. 2013). Due to the need for multiple batches in the human study, batch correction was performed using ComBat (Leek et al. 2012). No batch effects were observed for *C. elegans* studies and

326 detected intensities were used as is for statistical analyses. Intensities were generalized
327 log transformed prior to analysis.
328
329 **5. High-resolution metabolomic data analyses.**
330 **5.1. Human: analysis of LC-HRMS data.** Association of metabolite peaks with p-tau
331 levels were assessed using linear regression for metabolites detected in >80% of study
332 samples while controlling for sex, age and analysis batch.
333 Features associated with p-tau levels ($p < 0.05$) were analyzed for metabolic pathway
334 enrichment using mummichog (version 2.0.6) in Python (version 2.7) (Li et al. 2013).
335 In a sensitivity analysis, features associated with AD dementia vs. NC were examined
336 using the subset of features present in >20% of samples, reflecting a markedly lower
337 threshold for feature filtering compared to our previous analysis of AD (Niedzwiecki et al.
338 2020). Statistical analyses were conducted as previously described (Niedzwiecki et al.
339 2020).
340
341 **5.2. *C. elegans*: analysis of LC-HRMS data and overlap.** All feature tables were
342 processed as follows: first, the intensity of a metabolite peak in the samples was
343 compared to its intensity in the medium blank (M9 buffer). If the intensity was ≥ 1.5 times
344 the intensity in the blank in all samples, it was retained for subsequent analysis. Second,
345 if a metabolite peak was missing from fewer than 50% of the samples, it was replaced
346 with half the value of the minimum intensity measured in the samples. Features missing
347 from more than 50% of the samples were removed from downstream analysis. Third, the
348 filtered and imputed feature table was imported into MetaboAnalyst (Pang et al. 2020)

and normalized by generalized log transformation. Three different analyses were conducted using the processed *C. elegans* data:

1. Metabolic effects of aggregating tau protein. The filtered feature table was used to determine the metabolites associated with the aggregating worms by comparing aggregating to non-aggregating worms using multiple t-tests. Metabolites with $p < 0.05$ were analyzed for pathway analysis using mummichog hosted on MetaboAnalyst (Chong et al. 2018) using the *C. elegans* KEGG reference map.

2. Analysis of metabolites common to humans and *C. elegans* that are associated with tau protein. Plasma and CSF derived metabolites that were associated with CSF p-tau ($p < 0.05$) or neuronal expression in *C. elegans* ($p < 0.05$) were compared using KEGG ID annotations from pathway analysis. A metabolite was considered overlapping if it was significantly associated with tau protein in both species, was annotated with a KEGG ID, and the direction of association was concordant between worms and humans.

3. The metabolic effect of DDT in all three strains. The filtered feature table was used to determine: the metabolomic profile of DDT exposure in wildtype worms, the metabolomic profile of DDT exposure in the aggregating worms, and the metabolomic profile associated with the aggregating worms by comparing metabolite peaks from the aggregating and non-aggregating worms exposed to the vehicle control. For all analyses, we used t-tests to compare differences in mean intensities. Significant metabolite peaks were tested for pathway enrichment using mummichog on MetaboAnalyst and the *C. elegans* KEGG reference map.

6. Statistical analyses. Tests for significance were determined through one-way ANOVA and post-hoc Tukey's HSD test, unless stated otherwise. All data were analyzed in R (version 4.0.2) using RStudio (v1.1.456) unless otherwise stated. Code and data associated with worm assays can be found at: https://github.com/vrindakalia/DDT_tau_Celegans

Results

CSF and plasma metabolism associated with CSF p-tau levels. There were no significant differences in the distribution of age or gender between the three different diagnoses. Patients with AD and MCI had higher levels of p-tau measured in their CSF compared to controls (Table 1). Following data extraction and filtering, 6,028 metabolite peaks were detected and measured in the CSF of patients and 7,249 m/z features in plasma. After controlling for the age, sex, and batch of analysis, we found 225 metabolites in CSF (Figure 1 A) and 391 in plasma (Figure 1 C) that were associated with CSF levels of p-tau at $p < 0.05$. Pathway analysis of the CSF metabolites found pathways associated with glutamate metabolism, carnitine metabolism, lysine metabolism, saturated fatty acid metabolism, as well as metabolism of several amino acids (Figure 1 B), while pathways in plasma-derived were consistent with drug metabolism, carnitine metabolism, lysine metabolism, and pathways associated with energy production (Figure 1 D).

Changes in global metabolism associated with aggregating tau protein expression in *C. elegans*. HRM detected 19,380 metabolite peaks in *C. elegans* using the HILIC column with positive ionization mode. After blank filtration and imputation, 8,860 were

retained for further analysis. Metabolome wide association analysis found more than 900 m/z features that were significantly different ($p < 0.05$) between the aggregating and non-aggregating strain (Figure 1 E). Metabolites were tested for pathway enrichment using the KEGG *C. elegans* reference map, which identified changes in the tryptophan and arginine pathway, glycerophospholipid metabolism, lysine degradation, glutathione metabolism, as well as glutamate and glutamine metabolism implicating altered amino acid metabolism (Figure 1 F).

Metabolites associated with aggregating tau protein in both species. The analysis to determine metabolites associated with p-tau in both humans and *C. elegans* was conducted separately for CSF and plasma. Metabolite annotations from mummichog (Schymanksi level 3 confidence (Schymanski et al. 2014)) were then used to test for overlap with unique KEGG ID annotation. We identified 4 CSF-derived metabolites and 5 plasma-derived metabolites overlapping with metabolites from the aggregating tau *C. elegans* strain associated with CSF p-tau levels in the same direction (Figure 1 G - J).

Metabolites associated with AD dementia versus normal controls. Since common thresholds for feature filtering in metabolomics pre-processing pipelines may remove low-abundance exogenous chemicals of interest, we conducted a sensitivity analysis to identify plasma metabolites associated with AD (vs. NC) using a lower threshold for missingness (removal of features missing in >80% of samples) compared to our original study (>20%) (Supplemental Table 2). One feature elevated in AD, *m/z* 386.8946, could not be identified with MS/MS due to low abundance but had a unique match in the

417 METLIN database to 1,1-dichloro-2-(dihydroxy-4'-chlorophenyl)-2-(4'-
418 chlorophenyl)ethylene, a metabolite of DDT.
419
420 **DDT uptake in *C. elegans*.** The *C. elegans* cuticle is known to be a barrier against
421 absorption of toxicants (Hunt 2017). The nematode is known to possess CYP 450
422 enzymes, although their repertoire is not as extensive as in mammals (Harlow et al. 2018).
423 We evaluated if *C. elegans* can absorb and metabolize DDT by measuring the levels of
424 p,p'-DDT, p,p'-DDE, p,p'-DDD, o,p'-DDT, o,p'-DDE, and o,p'-DDD in worms using GC-
425 HRMS. In wildtype worms, exposure to 0.3, 3, and 30 μM DDT led to internal levels of
426 0.27, 0.49 and 1.3 picogram of p,p'-DDT in each worm, respectively (Figure 2 A). All
427 metabolites of p,p'-DDT were also detectable and measured in the transgenic strain. In
428 all strains exposed to 3 μM DDT, the levels of p,p'-DDE were about 5-10 times lower than
429 p,p'-DDT.
430
431 **Effect of DDT exposure on *C. elegans* size**. Assessment of TOF (length) and extinction
432 (optical density) at 46-50 hours post synchronization (~larval stage 4) revealed that the
433 aggregating strain were smaller and with lower density compared to the non-aggregating
434 and wildtype worms. Exposure to DDT reduced the size and density in all strains
435 assessed (Figure 2 B & C). Measurement at 70-72 hours post synchronization (young
436 adulthood) showed that both tau transgenic strains are smaller ($p < 0.0001$) than wildtype
437 worms, with the aggregating strains more severely affected. Exposure to DDT reduced
438 the size of all strains in a graded manner, with the aggregating strain exposed to DDT
439 being the smallest (Figure 2 D & E).

Effect of tau protein and DDT on swim behavior of *C. elegans*. The aggregating strain showed differences in wave initiation rate and travel speed compared to the wildtype worms (Figure 3 A & B). Exposure to DDT in the aggregating strain almost doubled the percentage of time the worms spent curling when swimming (average percentage of time spent curling in aggregating worms + solvent control was 1.13%, and in aggregating worms + DDT: 1.83%, $p < 0.001$, Figure 3 C). The aggregating strain showed a lower activity index (average activity index in non-aggregating strain was 388.6 and in aggregating strain was 286.6, $p < 0.01$) Figure 3 D), and a difference in time spent reversing and brushstroke ($p < 0.05$ Supplemental Figure 1) compared to wildtype worms. Exposure to DDT did not significantly alter any swim behavior in the wildtype or non-aggregating strain.

Effect of tau and DDT on mitochondrial respiration. Wildtype worms and the non-aggregating strain showed similar oxygen consumption profiles (Figure 4 A). The aggregating strain showed reduced rates of basal, maximal, spare, and non-mitochondrial oxygen consumption rate (OCR) when compared to the non-aggregating strain (Figure 4 B - E). Exposure to 3 μM DDT in the N2 and non-aggregating strain reduced OCR at all four states (Figure 4 A - E). Exposure to DDT in the aggregating strain significantly reduced basal OCR ($p < 0.05$, Figure 4 B). Other measures of respiration were also reduced due to DDT exposure in the aggregating strain however, none were significantly different at $p < 0.05$ (Figure 4 C - E).

463 **Metabolic response to DDT and tau protein.** All strains exposed to DDT showed lower
464 metabolite intensities using HILIC with positive ionization (Figure 5 A) and the other
465 modes: HILIC column under negative ESI and the C18 column under positive and
466 negative ESI (Supplemental Figure 2 - 4). A biplot of principal component (PC) 1 against
467 PC2 shows that the wildtype and non-aggregating strain cluster together while the strains
468 exposed to DDT clustered differently from the unexposed wildtype and non-aggregating
469 strain along PC1 (Figure 5 B). Levels of uric acid and adenosylselenohomocysteine were
470 elevated in all strains exposed to DDT (Figure 5 C). In wildtype worms, exposure to DDT
471 altered amino acids pathways (Figure 6). DDT exposure in the aggregating strain resulted
472 in altered amino acid pathways, TCA cycle metabolism and glyoxylate and dicarboxylate
473 metabolism (Figure 6).
474
475 **Effect of DDT exposure on learning.** There was no difference in learning determined
476 through the associative learning paradigm among the three strains. Further, exposure to
477 DDT did not show an effect on learning (Figure 7 A & B).
478
479 **Effect of DDT exposure on survival.** The non-aggregating and aggregating strains
480 exhibited a shorter lifespan compared to the wildtype worms (average lifespan in wildtype
481 worms was 24 days, in non-aggregating worms was 19.4 days, and in aggregating worms
482 was 8 days, $p < 0.0001$, Figure 7 C). Exposure to DDT does not alter the lifespan in
483 wildtype or the non-aggregating strain. In the aggregating strain, exposure to DDT slightly
484 rescued the reduction in lifespan in the strain (mean lifespan was 11.8 days), however,

485 the lifespan was still shorter than that of the non-aggregating and wildtype strain (Figure
486 7 C & D).
487
488 **Discussion**
489 Model organisms are a useful tool to understand age-related changes in biology
490 and pathology. A number of signaling pathways that act as master regulators of lifespan
491 are conserved in yeast, nematodes, flies, and mammals (Bishop et al. 2010). The use of
492 model systems has uncovered evolutionarily conserved pathways that regulate both
493 longevity and age-related changes in learning and memory (Bishop et al. 2010; Friedman
494 and Johnson 1988; Grotewiel et al. 2005; Kauffman et al. 2010; Kenyon et al. 1993; Klass
495 1977; Silva et al. 1998). We used the nematode *C. elegans* to study environmental
496 determinants of aging and cognitive function. The organism's short lifespan (2-3 weeks)
497 makes it ideal to study the process of aging and diseases associated with age, such as
498 AD (Ardiel and Rankin 2010; Arey and Murphy 2017; Jonsson et al. 2013; Link 2006). In
499 addition, *C. elegans* mitochondria show close structural and functional conservation to
500 mammalian mitochondria (Murfitt et al. 1976) and pathways of intermediary metabolism
501 are also highly conserved (O'Riordan and Burnell 1990). Thus, we attempted to find
502 similarities in systemic biochemistry associated with aggregating tau protein toxicity,
503 which is a pathological hallmark of AD, in humans and *C. elegans*.
504 Our group has previously reported plasma metabolites associated with AD in the
505 cohort studied herein (Niedzwiecki et al. 2020). The most significant (lowest p-value)
506 metabolite associated with CSF p-tau was a metabolite of the drug Rivastigmine, an
507 acetylcholinesterase inhibitor. This was also the top metabolite associated with AD in the

508 previous study. The plasma levels of glutamine were positively associated with levels of
509 CSF p-tau. Metabolomic profiling of the CSF showed a negative association between
510 CSF levels of p-tau and glutamine, contrary to the direction of the association found in
511 plasma. This could be the result of differential changes in the glutamate/glutamine cycle
512 in the central nervous system and the periphery. The CSF-derived metabolites associated
513 with p-tau levels are related to butanoate metabolism and carnitine shuttle pathways, both
514 of which are associated with mitochondrial function (Pettegrew et al. 2000; Rose et al.
515 2018).

516 Using a transgenic strain of *C. elegans* that expresses a mutant form of human tau
517 protein in all neurons, we observed changes in several metabolite peaks that were
518 associated with aggregating tau protein. Pathway analysis using these features revealed
519 changes in metabolic pathways that have previously been associated with
520 neurodegeneration and AD, including the glycerophospholipid pathway, and glyoxylate
521 and dicarboxylate metabolism (Frisardi et al. 2011; Yan et al. 2020)

522 The 4 metabolites associated with p-tau and overlapping between CSF
523 metabolites and worm metabolites were tyrosine, carnitine, cystine and N, N-
524 dimethylaniline N oxide. While we did not find information on the relationship between N,
525 N-dimethylaniline N oxide and neurodegeneration or AD, all three of the other metabolites
526 have been previously associated with AD. Several studies have reported lower levels of
527 tyrosine measured in the CSF of AD patients (Basun et al. 1990; Martinez et al. 1993).
528 An untargeted HRM analysis of CSF samples from MCI patients showed altered tyrosine
529 metabolism (Hajjar et al. 2020). A study of CSF from non-*APOE4* carriers in the early
530 stage of AD reported lower levels of carnitine in the CSF (Lodeiro et al. 2014). Another

study of CSF from AD patients found lower levels of free carnitine but increased levels of acylcarnitine suggesting impaired energy production through anaplerotic pathways (van der Velpen et al. 2019). We detected decreased levels of cystine in plasma, CSF, and worms. Cystine is the dimer form of cysteine, a sulfur containing amino acid that functions to reduce redox stress. Several studies have reported increased levels of cysteine in the brain, plasma, and CSF of AD patients (Czech et al. 2012; Mahajan et al. 2020; Trushina et al. 2013). This could be a result of increased conversion of cystine to cysteine to ameliorate oxidative stress.

Apart from cystine, the other metabolites associated with p-tau found to be overlapping between plasma and worms were lipoamide, diethylthiophosphoric acid, 11,12-dihydroxy-5Z,8Z,14Z-eicosatrienoic acid (11,12-DHET), and N-acetyl lysine. Lipoamide is the amide form of lipoic acid which is a naturally occurring disulfide compound that functions as a co-factor for mitochondrial bioenergetic enzymes. It has been proposed as a novel treatment for AD owing to the many functions it performs (Holmquist et al. 2007). Lipoic acid can increase acetylcholine production (Haugaard et al. 2000) and glucose uptake (Holmquist et al. 2007) and it is reported to improve peripheral insulin resistance and impaired glucose metabolism (Bitar et al. 2004; Lee et al. 2005; Thirunavukkarasu et al. 2004). Diethylthiophosphoric acid is a part of the aminobenzoate degradation pathway. Derivatives of aminobenzoic acid may have potential as drugs to inhibit acetylcholinesterase, thereby ameliorating the acetylcholine deficit present in AD (Shrivastava et al. 2019). 11,12-DHET derives from oxidation of arachidonic acid, a well-known precursor activated during inflammatory response. A study using strains of mice expressing Aβ and tau in the brain found increased levels of several

554 eicosanoids in the brain and in plasma of these mice (Tajima et al. 2013). In both human
555 plasma and worms we found higher levels of DHET, in line with previous findings. Finally,
556 altered lysine metabolism has been previously reported in cases of MCI compared to
557 cognitively normal individuals (Trushina et al. 2013) and lysine supplementation has been
558 proposed as a treatment strategy for AD (Kumar and Kumar 2019).

559 Neither the human nor *C. elegans* metabolome is fully curated, and non-targeted
560 metabolomics data includes many dietary, microbiome and environmental chemicals in
561 addition to those associated with endogenous metabolic pathways as presented here.
562 Although the results from this cross-species analysis should be interpreted with caution,
563 the concordance between several metabolites that have been previously associated with
564 AD provides support for using *C. elegans* as a model to study biochemical changes
565 associated with AD-related pathology. Further, the disruptions in evolutionarily conserved
566 pathways that are associated with AD-related related pathology offer great power for
567 mechanistic interpretation. Correlation between metabolites observed across species
568 could provide a means to identify overlapping central networks and interacting sub-
569 networks associated with AD-related pathology (Kalia et al. 2019). In the future, we plan
570 to use mutant strains and appropriate exposures to determine the role of these
571 metabolites in the aggregating tau protein related toxicity in *C. elegans*.

572 Untargeted HRM approaches allow us to study the effect of the exposome on
573 human health (Vermeulen et al. 2020). However, in untargeted HRM analyses, the
574 abundance of exogenously-derived parent compounds and their metabolites tend to be
575 orders of magnitude lower than endogenous chemicals (Rappaport et al. 2014) and may
576 not be present in all study participants. Thus, statistical approaches and thresholds need

577 to be adjusted to account for this lower abundance and prevalence of exogenous
578 chemicals in population studies. Therefore, we conducted a sensitivity analysis by
579 applying a lower threshold for feature filtering in our previous analysis of plasma-derived
580 features associated with AD. The analysis found higher levels of a halogenated
581 metabolite in the plasma of AD patients, which was putatively identified as a derivative of
582 the persistent pesticide DDT (Supplemental Table 2).

583 To investigate whether exposure to DDT can exacerbate tau protein toxicity, we
584 used a transgenic *C. elegans* strain that expresses human tau protein and a mutated tau
585 protein sequence that has a propensity to form tau protein aggregates. We also used a
586 transgenic strain to serve as control for the aggregating strain that expresses the same
587 human tau protein but the mutated tau protein sequence is not prone to aggregation.
588 These transgenes are expressed in all neurons of the worm driven through the *rab-3*
589 promotor (Fatouros et al. 2012).

590 The targeted GC-HRMS assay detected and measured several metabolites of p,p'-
591 DDT in worms exposed to the pesticide, suggesting that the pesticide is not only absorbed
592 but also biotransformed in the nematode, supporting the use of this model to study the
593 toxic effects of DDT. Previously, Mahmood (2016) found that exposure to 1 μg/mL of DDT
594 (~2.8 μM) had a mild inhibitory effect on pharyngeal pumping, while this dose had no
595 effect on brood size. A survey of serum samples analyzed for levels of p,p'-DDT
596 conducted by NHANES showed a wide range of the pesticide in the blood of the American
597 population, and levels of p,p'-DDT measured increased with increasing age. Among those
598 aged 12-19 years in the survey, the geometric mean of lipid adjusted serum p,p'-DDT
599 level was less than 5 ng/g lipid (CDC 2020). Assuming the wet mass of a single worm is

1 μg (Muschiol et al. 2009), exposure to 3 μM DDT using our paradigm resulted in a mean level of ~0.5 ng/g wet weight of *C. elegans*. Thus, we exposed the wildtype, aggregating, and non-aggregating strains to 3 μM DDT during development and measured the effect of exposure on swim behavior, respiration, growth, metabolism, learning, and lifespan.

Similar to previous findings (Fatouros et al. 2012), we observed that the aggregating strain travels slower than the wildtype worms. The aggregating strain also showed a reduced wave initiation rate, which is akin to a swimming stroke rate (Restif et al. 2014), compared with the non-aggregating and wildtype strain. Additionally, the aggregating strain had a lower overall activity index compared with the non-aggregating and wildtype strain. Exposure to DDT significantly increased the amount of time the aggregating strain spent curling. The curling phenotype has been used to screen for motility defects in worms. A recent screen for curling identified the *bcat-1* gene to be associated with a Parkinson's-like phenotype and knockdown of the gene transcript showed altered mitochondrial function (Mor et al. 2020). The curling phenotype has also been used to ascertain dopaminergic toxicity due to the complex I inhibitor, MPP^+ (Braungart et al. 2004; Richardson et al. 2005).

We observed that the aggregating strain has severely impaired mitochondrial respiration, with diminished basal and maximal respiration compared with the non-aggregating strain. Several *in vitro* and *in vivo* studies have shown that aggregating tau protein can inhibit complex I and V of the mitochondria (David et al. 2005; Kim and Chan 2001; Lasagna-Reeves et al. 2011). Tau protein can alter the mitochondrial membrane potential, cause activation of the apoptotic-related caspase-9, and impede energy production (Lasagna-Reeves et al. 2011; Shafiei et al. 2017). Furthermore, disintegration

of tau protein can lead to disturbed transport of mitochondria across microtubules and mitochondrial fission-fusion dynamics (Eckert et al. 2014; Fatouros et al. 2012).

Exposure to DDT in the wildtype and non-aggregating strain severely impaired mitochondrial respiration at baseline and in the uncoupled state (FCCP). Several *in vitro* and *in vivo* studies have reported an inhibitory effect of DDT on mitochondrial function and ATP production, but none have reported this in *C. elegans*. DDT is known to inhibit complex II, III, and V of the electron transport chain and it depresses the mitochondrial membrane potential (Elmore and La Merrill 2019; Moreno and Madeira 1991). In rats, exposure to DDT reduced the number of mitochondria measured in the liver and altered fatty acid metabolism (Liu et al. 2017), an effect that would be consistent with the overall decrease in OCR under all states measured. We note that this overall decrease in oxidative phosphorylation activity is also unlikely to be attributable to decreased motility since exposure to DDT did not affect the swimming behavior of wildtype worms, reinforcing the interpretation that DDT may directly affect either mitochondrial content and/or respiratory chain activity.

We found that the aggregating strain was smaller in size at larval stage 4 and in adulthood compared to the non-aggregating strain. This could be attributed to reduced energy production and biomass accumulation due to mitochondrial inhibition. When exposed to DDT, there was no difference in size between the aggregating and non-aggregating strains at larval stage 4; however, in adulthood, DDT reduced the size of the aggregating strain more than in the non-aggregating strain. It is likely that the additional insult on the mitochondria by DDT restricts growth which was only detectable following the initiation of reproductive capacity.

HRM found several metabolites to be altered in worms following DDT exposure. Levels of several amino acids were reduced along with intermediates of the TCA cycle and branched chain amino acid metabolism. Uric acid was increased in all strains exposed to DDT (Figure 6 A). Uric acid is the end product of purine metabolism and has anti-oxidant properties since it can scavenge free radicals and prevent lipid peroxidation (Hooper et al. 1998). High levels of uric acid have been reported to induce stress response pathways in *C. elegans* by increasing levels of the DAF-16/FOXO and SKN-1/NRF-2 transcripts (Wan et al. 2020). Levels of adenosylselenohomocysteine were also found to be increased in all strains exposed to DDT and in the aggregating strain (Figure 6 B). Thioredoxin reductase-1 (TrxR-1) is the only selenium containing protein in *C. elegans* (Rohn et al. 2018). An elevated seleno-metabolite suggests increased levels of TrxR-1 in response to oxidative stress induced by DDT exposure and tau protein aggregation.

The aggregating strain did not show any difference in their ability to learn following an associative training paradigm, compared to the non-aggregating or wildtype strain. These findings are similar to those made by Wang and colleagues (2018). Exposure to DDT did not affect this ability to learn in either strain using the associative learning assay.

We found that the non-aggregating and aggregating strains have a reduced lifespan compared to wildtype worms, replicating previous findings (Wang et al. 2018). The proteotoxicity and reduced respiratory rate in the aggregating strain could explain this observation (Zarse et al. 2007). Interestingly, exposure to DDT did not change the mean lifespan in wildtype or non-aggregating worms but it slightly increased the mean lifespan of the aggregating strain. This finding is surprising but given that the exposure occurred

669 developmentally, it hints to the activation of mitohormetic pathways which could turn on
670 lifespan extension pathways (Maglioni et al. 2019), like the mitochondrial unfolded protein
671 response (UPR^{mt}) pathway. However, the extension in lifespan was not large enough to
672 be as much or more than the lifespan of the non-aggregating or wildtype strain. It is also
673 possible that, while mitochondrial inhibition by aggregating tau protein alone does not
674 induce the UPR^{mt} pathways, the mitochondrial stress induced by DDT during
675 development produces an antagonistic effect which induces stress response pathways
676 (Wytock et al. 2020).

677 While we present evidence that supports the use of *C. elegans* as a model to study
678 whether DDT can exacerbate tau protein toxicity, our study has several limitations. In
679 insects and mammals, DDT inhibits voltage-gated sodium channel inactivation and
680 stabilizes the open state of sodium channels, causing prolonged channel opening
681 (Bloomquist 1996; Narahashi 2000). The *C. elegans* genome does not encode for
682 voltage-gated sodium channels (Hobert 2018), thus DDT does not produce neurotoxicity
683 through this mechanism in the nematode. Thus, we were unable to measure any
684 interaction tau protein aggregation may have with altered neuronal excitability elicited by
685 DDT in mammalian neurons. Furthermore, in the transgenic model we chose, we were
686 unable to control the level of tau protein aggregates expressed in the neurons. It is
687 possible that the severe tau protein aggregation toxicity obscured effects of DDT
688 exposure and its proteotoxic effects. The interactions between the two insults may
689 become more apparent when lower levels of the aggregates are expressed.

690 Despite these limitations, we provide evidence that support the use of *C. elegans* as a
691 model to study gene- environment interactions. We provide evidence that DDT is taken

up and biotransformed by *C. elegans*. In wildtype worms, DDT restricts growth, as measured by size, and reduces mitochondrial respiration. DDT produces major changes in global metabolism, including pathways related to neurotransmitter precursors and other amino acid metabolism. In transgenic worms that express an aggregating form of human tau protein in all neurons, DDT restricts growth even further and reduces the basal respiration rate. Aggregating tau worms exposed to DDT spend more time curling when swimming, a known mitochondrial toxicity phenotype. Further, DDT exposure affects the metabolism of several amino acids, the TCA cycle, and the glyoxylate and dicarboxylate metabolic pathway. Our data suggest that exposure to DDT likely exacerbates the mitochondrial inhibitory effects of aggregating tau protein in *C. elegans*. Additionally, the concordance between several metabolites that have been previously associated with AD provides validity to using *C. elegans* as a model to study biochemical changes associated with AD-related pathology. In the future, using transgenic *C. elegans* strains, we will perform systematic analyses of the environmental drivers of AD that can lead to interventional strategies aimed at preventing or treating the disease.

Acknowledgements

G.W.M is supported by NIH grants RF1AG066107, R01AG067501, U2C ES030163, R01ES023839, M.L.B. is supported by NIEHS grant T32ES007732, D.I.W. is supported by NIEHS grant U2C ES030859 and K.E.M. is supported by NEIHS grant T32ES007272.

References

Albert MS, DeKosky ST, Dickson D, Dubois B, Feldman HH, Fox NC, et al. 2011. The diagnosis of mild cognitive impairment due to Alzheimer's disease: recommendations from the National Institute on Aging-Alzheimer's Association workgroups on diagnostic guidelines for Alzheimer's disease. Alzheimers Dement 7:270–279; doi:10.1016/j.jalz.2011.03.008.

Ardiel EL, Rankin CH. 2010. An elegant mind: Learning and memory in Caenorhabditis elegans. Learn Mem 17:191–201; doi:10.1101/lm.960510.

Arey RN, Murphy CT. 2017. Conserved regulators of cognitive aging: From Worms to Humans. Behav Brain Res 322:299–310; doi:10.1016/j.bbr.2016.06.035.

Basun H, Forssell LG, Almkvist O, Cowburn RF, Eklöf R, Winblad B, et al. 1990. Amino acid concentrations in cerebrospinal fluid and plasma in Alzheimer's disease and healthy control subjects. J Neural Transm Gen Sect 2:295–304; doi:10.1007/BF02252924.

Bischof GN, Park DC. 2015. Obesity and Aging: Consequences for Cognition, Brain Structure, and Brain Function. Psychosom Med 77:697–709; doi:10.1097/PSY.0000000000000212.

Bishop NA, Lu T, Yankner BA. 2010. Neural mechanisms of ageing and cognitive decline. Nature 464:529–535; doi:10.1038/nature08983.

Bitar MS, Wahid S, Pilcher CW, Al-Saleh E, Al-Mulla F. 2004. Alpha-lipoic acid mitigates insulin resistance in Goto-Kakizaki rats. Hormone and Metabolic Research 36: 542–549.

Bloomquist JR. 1996. Ion channels as targets for insecticides. Annu Rev Entomol 41:163–190; doi:10.1146/annurev.en.41.010196.001115.

Boyd WA, Smith MV, Co CA, Pirone JR, Rice JR, Shockley KR, et al. 2016. Developmental Effects of the ToxCast™ Phase I and Phase II Chemicals in Caenorhabditis elegans and Corresponding Responses in Zebrafish, Rats, and Rabbits. Environ Health Perspect 124:586–593; doi:10.1289/ehp.1409645.

Bradner JM, Kalia V, Lau FK, Sharma M, Bucher ML, Johnson M, et al. 2021. Genetic or Toxicant-Induced Disruption of Vesicular Monoamine Storage and Global Metabolic Profiling in Caenorhabditis elegans. Toxicological Sciences; doi:10.1093/toxsci/kfab011.

Braungart E, Gerlach M, Riederer P, Baumeister R, Hoener MC. 2004. Caenorhabditis elegans MPP+ Model of Parkinson's Disease for High-Throughput Drug Screenings. NDD 1:175–183; doi:10.1159/000080983.

Brenner S. 1974. The genetics of Caenorhabditis elegans. Genetics 77: 71–94.

C. elegans Sequencing Consortium. 1998. Genome sequence of the nematode C. elegans: a platform for investigating biology. Science 282:2012–2018; doi:10.1126/science.282.5396.2012.

Chong J, Soufan O, Li C, Caraus I, Li S, Bourque G, et al. 2018. MetaboAnalyst 4.0: towards more transparent and integrative metabolomics analysis. Nucleic Acids Research 46:W486–W494; doi:10.1093/nar/gky310.

Cole RD, Anderson GL, Williams PL. 2004. The nematode Caenorhabditis elegans as a model of organophosphate-induced mammalian neurotoxicity. Toxicol Appl Pharmacol 194:248–256; doi:10.1016/j.taap.2003.09.013.

Corsi AK, Wightman B, Chalfie M. 2015. A Transparent window into biology: A primer on Caenorhabditis elegans. WormBook 1–31; doi:10.1895/wormbook.1.177.1.

Czech C, Berndt P, Busch K, Schmitz O, Wiemer J, Most V, et al. 2012. Metabolite profiling of Alzheimer's disease cerebrospinal fluid. PloS one 7: e31501.

David DC, Hauptmann S, Scherping I, Schuessel K, Keil U, Rizzu P, et al. 2005. Proteomic and Functional Analyses Reveal a Mitochondrial Dysfunction in P301L Tau Transgenic Mice. J Biol Chem 280:23802–23814; doi:10.1074/jbc.M500356200.

de la Monte SM, Wands JR. 2008. Alzheimer's disease is type 3 diabetes-evidence reviewed. J Diabetes Sci Technol 2:1101–1113; doi:10.1177/193229680800200619.

DeKosky ST, Gandy S. 2014. Environmental Exposures and the Risk for Alzheimer Disease: Can We Identify the Smoking Guns? JAMA Neurol 71:273–275; doi:10.1001/jamaneurol.2013.6031.

Eckert A, Nisbet R, Grimm A, Götz J. 2014. March separate, strike together--role of phosphorylated TAU in mitochondrial dysfunction in Alzheimer's disease. Biochim Biophys Acta 1842:1258–1266; doi:10.1016/j.bbadis.2013.08.013.

Elmore SE, La Merrill MA. 2019. Oxidative Phosphorylation Impairment by DDT and DDE. Front Endocrinol 10; doi:10.3389/fendo.2019.00122.

Fatouros C, Pir GJ, Biernat J, Koushika SP, Mandelkow E, Mandelkow E-M, et al. 2012. Inhibition of tau aggregation in a novel Caenorhabditis elegans model of tauopathy mitigates proteotoxicity. Hum Mol Genet 21:3587–3603; doi:10.1093/hmg/dds190.

Friedman DB, Johnson TE. 1988. A mutation in the age-1 gene in Caenorhabditis elegans lengthens life and reduces hermaphrodite fertility. Genetics 118: 75–86.

Frisardi V, Panza F, Seripa D, Farooqui T, Farooqui AA. 2011. Glycerophospholipids and glycerophospholipid-derived lipid mediators: a complex meshwork in Alzheimer's disease pathology. Prog Lipid Res 50:313–330; doi:10.1016/j.plipres.2011.06.001.

777 Go Y-M, Walker DI, Liang Y, Uppal K, Soltow QA, Tran V, et al. 2015. Reference Standardization
778 for Mass Spectrometry and High-resolution Metabolomics Applications to Exposome
779 Research. Toxicol Sci 148:531–543; doi:10.1093/toxsci/kfv198.

780 Grotewiel MS, Martin I, Bhandari P, Cook-Wiens E. 2005. Functional senescence in Drosophila
781 melanogaster. Ageing Res Rev 4:372–397; doi:10.1016/j.arr.2005.04.001.

782 Hajjar I, Liu C, Jones DP, Uppal K. 2020. Untargeted metabolomics reveal dysregulations in
783 sugar, methionine, and tyrosine pathways in the prodromal state of AD. Alzheimer's &
784 Dementia: Diagnosis, Assessment & Disease Monitoring 12:e12064;
785 doi:https://doi.org/10.1002/dad2.12064.

786 Harlow PH, Perry SJ, Stevens AJ, Flemming AJ. 2018. Comparative metabolism of xenobiotic
787 chemicals by cytochrome P450s in the nematode Caenorhabditis elegans. Scientific
788 Reports 8:13333; doi:10.1038/s41598-018-31215-w.

789 Harlow PH, Perry SJ, Widdison S, Daniels S, Bondo E, Lamberth C, et al. 2016. The nematode
790 Caenorhabditis elegans as a tool to predict chemical activity on mammalian
791 development and identify mechanisms influencing toxicological outcome. Sci Rep
792 6:22965; doi:10.1038/srep22965.

793 Haugaard N, Levin RM, Surname F. 2000. Regulation of the activity of choline acetyl transferase
794 by lipoic acid. Molecular and Cellular Biochemistry 213: 61–63.

795 Hobert O. 2018. The neuronal genome of Caenorhabditis elegans. In: *WormBook: The Online*
796 *Review of C. elegans Biology [Internet]*. WormBook.

797 Holmquist L, Stuchbury G, Berbaum K, Muscat S, Young S, Hager K, et al. 2007. Lipoic acid as a
798 novel treatment for Alzheimer's disease and related dementias. Pharmacology &
799 Therapeutics 113:154–164; doi:10.1016/j.pharmthera.2006.07.001.

800 Hooper DC, Spitsin S, Kean RB, Champion JM, Dickson GM, Chaudhry I, et al. 1998. Uric acid, a
801 natural scavenger of peroxynitrite, in experimental allergic encephalomyelitis and
802 multiple sclerosis. PNAS 95:675–680; doi:10.1073/pnas.95.2.675.

803 Howell JC, Watts KD, Parker MW, Wu J, Kollhoff A, Wingo TS, et al. 2017. Race modifies the
804 relationship between cognition and Alzheimer's disease cerebrospinal fluid biomarkers.
805 Alzheimers Res Ther 9; doi:10.1186/s13195-017-0315-1.

806 Hu WT, Watts KD, Shaw LM, Howell JC, Trojanowski JQ, Basra S, et al. 2015. CSF beta-amyloid 1-
807 42 - what are we measuring in Alzheimer's disease? Ann Clin Transl Neurol 2:131–139;
808 doi:10.1002/acn3.160.

809 Hunt PR. 2017. The C. elegans model in toxicity testing. J Appl Toxicol 37:50–59;
810 doi:10.1002/jat.3357.

811 Hunt PR, Olejnik N, Sprando RL. 2012. Toxicity ranking of heavy metals with screening method
812 using adult Caenorhabditis elegans and propidium iodide replicates toxicity ranking in
813 rat. Food Chem Toxicol 50:3280–3290; doi:10.1016/j.fct.2012.06.051.

814 Hunt PR, Son TG, Wilson MA, Yu Q-S, Wood WH, Zhang Y, et al. 2011. Extension of Lifespan in C.
815 elegans by Naphthoquinones That Act through Stress Hormesis Mechanisms. PLOS ONE
816 6:e21922; doi:10.1371/journal.pone.0021922.

817 Jonsson T, Stefansson H, Steinberg S, Jonsdottir I, Jonsson PV, Snaedal J, et al. 2013. Variant of
818 TREM2 associated with the risk of Alzheimer's disease. N Engl J Med 368:107–116;
819 doi:10.1056/NEJMoa1211103.

820 Kaletta T, Hengartner MO. 2006. Finding function in novel targets: C. elegans as a model
821 organism. Nat Rev Drug Discov 5:387–398; doi:10.1038/nrd2031.

822 Kalia V, Jones DP, Miller GW. 2019. Networks at the nexus of systems biology and the
823 exposome. Current Opinion in Toxicology; doi:10.1016/j.cotox.2019.03.008.

824 Kauffman A, Parsons L, Stein G, Wills A, Kaletsky R, Murphy C. 2011. C. elegans positive
825 butanone learning, short-term, and long-term associative memory assays. J Vis Exp;
826 doi:10.3791/2490.

827 Kauffman AL, Ashraf JM, Corces-Zimmerman MR, Landis JN, Murphy CT. 2010. Insulin Signaling
828 and Dietary Restriction Differentially Influence the Decline of Learning and Memory with
829 Age. PLOS Biology 8:e1000372; doi:10.1371/journal.pbio.1000372.

830 Kenyon C, Chang J, Gensch E, Rudner A, Tabtiang R. 1993. A C. elegans mutant that lives twice
831 as long as wild type. Nature 366:461–464; doi:10.1038/366461a0.

832 Kim GW, Chan PH. 2001. Oxidative Stress and Neuronal DNA Fragmentation Mediate Age-
833 Dependent Vulnerability to the Mitochondrial Toxin, 3-Nitropropionic Acid, in the
834 Mouse Striatum. Neurobiology of Disease 8:114–126; doi:10.1006/nbdi.2000.0327.

835 Klass MR. 1977. Aging in the nematode Caenorhabditis elegans: major biological and
836 environmental factors influencing life span. Mech Ageing Dev 6: 413–429.

837 Koopman M, Michels H, Dancy BM, Kamble R, Mouchiroud L, Auwerx J, et al. 2016. A screening-
838 based platform for the assessment of cellular respiration in Caenorhabditis elegans. Nat
839 Protocols 11:1798–1816; doi:10.1038/nprot.2016.106.

840 Kumar D, Kumar P. 2019. An In-Silico Investigation of Key Lysine Residues and Their Selection
841 for Clearing off Aβ and Holo-AβPP Through Ubiquitination. Interdiscip Sci 11:584–596;
842 doi:10.1007/s12539-018-0307-2.

843 Lasagna-Reeves CA, Castillo-Carranza DL, Sengupta U, Clos AL, Jackson GR, Kayed R. 2011. Tau
844 oligomers impair memory and induce synaptic and mitochondrial dysfunction in wild-
845 type mice. Molecular Neurodegeneration 6:39; doi:10.1186/1750-1326-6-39.

846 Lee WJ, Song K-H, Koh EH, Won JC, Kim HS, Park H-S, et al. 2005. α-Lipoic acid increases insulin
847 sensitivity by activating AMPK in skeletal muscle. Biochemical and biophysical research
848 communications 332: 885–891.

849 Leek JT, Johnson WE, Parker HS, Jaffe AE, Storey JD. 2012. The sva package for removing batch
850 effects and other unwanted variation in high-throughput experiments. Bioinformatics
851 28:882–883; doi:10.1093/bioinformatics/bts034.

852 Li S, Park Y, Duraisingham S, Strobel FH, Khan N, Soltow QA, et al. 2013. Predicting network
853 activity from high throughput metabolomics. PLoS computational biology 9: e1003123.

854 Link CD. 2006. C. elegans models of age-associated neurodegenerative diseases: Lessons from
855 transgenic worm models of Alzheimer's disease. Experimental Gerontology 41:1007–
856 1013; doi:10.1016/j.exger.2006.06.059.

857 Liu KH, Nellis M, Uppal K, Ma C, Tran V, Liang Y, et al. 2020. Reference Standardization for
858 Quantification and Harmonization of Large-Scale Metabolomics. Anal Chem 92:8836–
859 8844; doi:10.1021/acs.analchem.0c00338.

860 Liu Q, Wang Q, Xu C, Shao W, Zhang C, Liu H, et al. 2017. Organochloride pesticides impaired
861 mitochondrial function in hepatocytes and aggravated disorders of fatty acid
862 metabolism. Scientific Reports 7:46339; doi:10.1038/srep46339.

863 Lodeiro M, Ibáñez C, Cifuentes A, Simó C, Cedazo-Mínguez Á. 2014. Decreased cerebrospinal
864 fluid levels of L-carnitine in non-apolipoprotein E4 carriers at early stages of Alzheimer's
865 disease. J Alzheimers Dis 41:223–232; doi:10.3233/JAD-132063.

866 Maglioni S, Mello DF, Schiavi A, Meyer JN, Ventura N. 2019. Mitochondrial bioenergetic changes
867 during development as an indicator of C. elegans health-span. Aging (Albany NY)
868 11:6535–6554; doi:10.18632/aging.102208.

869 Mahajan UV, Varma VR, Griswold ME, Blackshear CT, An Y, Oommen AM, et al. 2020.
870 Correction: Dysregulation of multiple metabolic networks related to brain
871 transmethylation and polyamine pathways in Alzheimer disease: A targeted
872 metabolomic and transcriptomic study. PLOS Medicine 17:e1003439;
873 doi:10.1371/journal.pmed.1003439.

874 Mahmood SM. 2016. Toxicological and Physiological Effects of DDT on Caenorhabditis elegans.
875 Ibn AL- Haitham Journal For Pure and Applied Science 24.

876 Martinez M, Frank A, Diez-Tejedor E, Hernanz A. 1993. Amino acid concentrations in
877 cerebrospinal fluid and serum in Alzheimer's disease and vascular dementia. J Neural
878 Transm Gen Sect 6:1–9; doi:10.1007/BF02252617.

879 Matthews KA, Xu W, Gaglioti AH, Holt JB, Croft JB, Mack D, et al. 2019. Racial and ethnic
880 estimates of Alzheimer's disease and related dementias in the United States (2015–
881 2060) in adults aged ≥65 years. Alzheimer's & Dementia: The Journal of the Alzheimer's
882 Association 15:17–24; doi:10.1016/j.jalz.2018.06.3063.

883 McKhann GM, Knopman DS, Chertkow H, Hyman BT, Jack CR, Kawas CH, et al. 2011. The
884 diagnosis of dementia due to Alzheimer's disease: recommendations from the National
885 Institute on Aging-Alzheimer's Association workgroups on diagnostic guidelines for
886 Alzheimer's disease. Alzheimers Dement 7:263–269; doi:10.1016/j.jalz.2011.03.005.

887 Middendorf PJ, Dusenbery DB. 1993. Fluoroacetic Acid Is a Potent and Specific Inhibitor of
888 Reproduction in the Nematode Caenorhabditis elegans. J Nematol 25: 573–577.

889 Mor DE, Sohrabi S, Kaletsky R, Keyes W, Tartici A, Kalia V, et al. 2020. Metformin rescues
890 Parkinson's disease phenotypes caused by hyperactive mitochondria. PNAS;
891 doi:10.1073/pnas.2009838117.

892 Moreno AJ, Madeira VM. 1991. Mitochondrial bioenergetics as affected by DDT. Biochimica et
893 Biophysica Acta (BBA)-Bioenergetics 1060: 166–174.

894 Murfitt RR, Vogel K, Sanadi DR. 1976. Characterization of the mitochondria of the free-living
895 nematode, caenorhabditis elegans. Comparative Biochemistry and Physiology Part B:
896 Comparative Biochemistry 53:423–430; doi:10.1016/0305-0491(76)90191-7.

897 Muschiol D, Schroeder F, Traunspurger W. 2009. Life cycle and population growth rate of
898 Caenorhabditis elegans studied by a new method. BMC Ecol 9:14; doi:10.1186/1472-
899 6785-9-14.

900 Narahashi T. 2000. Neuroreceptors and ion channels as the basis for drug action: past, present,
901 and future. J Pharmacol Exp Ther 294: 1–26.

902 National Report on Human Exposure to Environmental Chemicals | CDC. 2020. Available:
903 https://www.cdc.gov/exposurereport/index.html [accessed 27 November 2020].

904 Needham LL, Grandjean P, Heinzow B, Jørgensen PJ, Nielsen F, Patterson DG, et al. 2011.
905 Partition of Environmental Chemicals between Maternal and Fetal Blood and Tissues.
906 Environ Sci Technol 45:1121–1126; doi:10.1021/es1019614.

907 Nichols E, Szoeke CEI, Vollset SE, Abbasi N, Abd-Allah F, Abdela J, et al. 2019. Global, regional,
908 and national burden of Alzheimer's disease and other dementias, 1990–2016: a
909 systematic analysis for the Global Burden of Disease Study 2016. The Lancet Neurology
910 18:88–106; doi:10.1016/S1474-4422(18)30403-4.

911 Niedzwiecki MM, Walker DI, Howell JC, Watts KD, Jones DP, Miller GW, et al. 2020. High-
912 resolution metabolomic profiling of Alzheimer's disease in plasma. Annals of Clinical and
913 Translational Neurology 7:36–45; doi:10.1002/acn3.50956.

914 O'Riordan VB, Burnell AM. 1990. Intermediary metabolism in the dauer larva of the nematode
915 Caenorhabditis elegans—II. The glyoxylate cycle and fatty-acid oxidation. Comparative
916 Biochemistry and Physiology Part B: Comparative Biochemistry 95:125–130;
917 doi:10.1016/0305-0491(90)90258-U.

918 Ossenkoppele R, Schonhaut DR, Baker SL, O'Neil JP, Janabi M, Ghosh PM, et al. 2015. Tau,
919 amyloid, and hypometabolism in a patient with posterior cortical atrophy. Ann Neurol
920 77:338–342; doi:10.1002/ana.24321.

921 Ossenkoppele R, Schonhaut DR, Schöll M, Lockhart SN, Ayakta N, Baker SL, et al. 2016. Tau PET
922 patterns mirror clinical and neuroanatomical variability in Alzheimer's disease. Brain
923 139:1551–1567; doi:10.1093/brain/aww027.

924 Pang Z, Chong J, Li S, Xia J. 2020. MetaboAnalystR 3.0: Toward an Optimized Workflow for
925 Global Metabolomics. Metabolites 10:186; doi:10.3390/metabo10050186.

926 Park YH, Lee K, Soltow QA, Strobel FH, Brigham KL, Parker RE, et al. 2012. High-performance
927 metabolic profiling of plasma from seven mammalian species for simultaneous
928 environmental chemical surveillance and bioeffect monitoring. Toxicology 295:47–55;
929 doi:10.1016/j.tox.2012.02.007.

930 Pérez MJ, Jara C, Quintanilla RA. 2018. Contribution of Tau Pathology to Mitochondrial
931 Impairment in Neurodegeneration. Front Neurosci 12; doi:10.3389/fnins.2018.00441.

932 Pettegrew JW, Levine J, McClure RJ. 2000. Acetyl- L -carnitine physical-chemical, metabolic, and
933 therapeutic properties: relevance for its mode of action in Alzheimer's disease and
934 geriatric depression. Molecular Psychiatry 5:616–632; doi:10.1038/sj.mp.4000805.

935 Rappaport SM, Barupal DK, Wishart D, Vineis P, Scalbert A. 2014. The blood exposome and its
936 role in discovering causes of disease. Environ Health Perspect 122:769–774;
937 doi:10.1289/ehp.1308015.

938 Restif C, Ibanez-Ventoso C, Vora MM, Guo S, Metaxas D, Driscoll M. 2014. CeleST: computer
939 vision software for quantitative analysis of C. elegans swim behavior reveals novel
940 features of locomotion. PLoS Comput Biol 10:e1003702;
941 doi:10.1371/journal.pcbi.1003702.

942 Richardson JR, Quan Y, Sherer TB, Greenamyre JT, Miller GW. 2005. Paraquat neurotoxicity is
943 distinct from that of MPTP and rotenone. Toxicol Sci 88:193–201;
944 doi:10.1093/toxsci/kfi304.

945 Richardson JR, Roy A, Shalat SL, Stein RT von, Hossain MM, Buckley B, et al. 2014. Elevated
946 Serum Pesticide Levels and Risk for Alzheimer Disease. JAMA Neurol 71:284–290;
947 doi:10.1001/jamaneurol.2013.6030.

948 Rohn I, Marschall TA, Kroepfl N, Jensen KB, Aschner M, Tuck S, et al. 2018. Selenium species-
949 dependent toxicity, bioavailability and metabolic transformations in Caenorhabditis
950 elegans. Metallomics 10:818–827; doi:10.1039/c8mt00066b.

951 Rose S, Bennuri SC, Davis JE, Wynne R, Slattery JC, Tippett M, et al. 2018. Butyrate enhances
952 mitochondrial function during oxidative stress in cell lines from boys with autism.
953 Translational Psychiatry 8:1–17; doi:10.1038/s41398-017-0089-z.

954 Schymanski EL, Jeon J, Gulde R, Fenner K, Ruff M, Singer HP, et al. 2014. Identifying small
955 molecules via high resolution mass spectrometry: communicating confidence. Environ
956 Sci Technol 48:2097–8; doi:10.1021/es5002105.

957 Shafiei SS, Guerrero-Muñoz MJ, Castillo-Carranza DL. 2017. Tau Oligomers: Cytotoxicity,
958 Propagation, and Mitochondrial Damage. Front Aging Neurosci 9;
959 doi:10.3389/fnagi.2017.00083.

960 Shrivastava SK, Sinha SK, Srivastava P, Tripathi PN, Sharma P, Tripathi MK, et al. 2019. Design
961 and development of novel p-aminobenzoic acid derivatives as potential cholinesterase
962 inhibitors for the treatment of Alzheimer's disease. Bioorg Chem 82:211–223;
963 doi:10.1016/j.bioorg.2018.10.009.

964 Silva AJ, Kogan JH, Frankland PW, Kida S. 1998. Creb and Memory. Annual Review of
965 Neuroscience 21:127–148; doi:10.1146/annurev.neuro.21.1.127.

966 Soltow QA, Strobel FH, Mansfield KG, Wachtman L, Park Y, Jones DP. 2013. High-performance
967 metabolic profiling with dual chromatography-Fourier-transform mass spectrometry
968 (DC-FTMS) for study of the exposome. Metabolomics 9:S132–S143; doi:10.1007/s11306-
969 011-0332-1.

970 Tajima Y, Ishikawa M, Maekawa K, Murayama M, Senoo Y, Nishimaki-Mogami T, et al. 2013.
971 Lipidomic analysis of brain tissues and plasma in a mouse model expressing mutated
972 human amyloid precursor protein/tau for Alzheimer's disease. Lipids Health Dis 12:68;
973 doi:10.1186/1476-511X-12-68.

974 Thirunavukkarasu V, Nandhini AA, Anuradha CV. 2004. Lipoic acid attenuates hypertension and
975 improves insulin sensitivity, kallikrein activity and nitrite levels in high fructose-fed rats.
976 Journal of Comparative Physiology B 174: 587–592.

977 Trushina E, Dutta T, Persson X-MT, Mielke MM, Petersen RC. 2013. Identification of altered
978 metabolic pathways in plasma and CSF in mild cognitive impairment and Alzheimer's
979 disease using metabolomics. PLoS One 8:e63644; doi:10.1371/journal.pone.0063644.

980 Turusov V, Rakitsky V, Tomatis L. 2002. Dichlorodiphenyltrichloroethane (DDT): ubiquity,
981 persistence, and risks. Environ Health Perspect 110: 125–128.

982 Uppal K, Soltow QA, Strobel FH, Pittard WS, Gernert KM, Yu T, et al. 2013. xMSanalyzer:
983 automated pipeline for improved feature detection and downstream analysis of large-
984 scale, non-targeted metabolomics data. BMC Bioinformatics 14:15; doi:10.1186/1471-
985 2105-14-15.

986 Van Cauwenberghe C, Van Broeckhoven C, Sleegers K. 2016. The genetic landscape of
987 Alzheimer disease: clinical implications and perspectives. Genet Med 18:421–430;
988 doi:10.1038/gim.2015.117.

989 van den Berg H, Manuweera G, Konradsen F. 2017. Global trends in the production and use of
990 DDT for control of malaria and other vector-borne diseases. Malaria Journal 16:401;
991 doi:10.1186/s12936-017-2050-2.

992 van der Velpen V, Teav T, Gallart-Ayala H, Mehl F, Konz I, Clark C, et al. 2019. Systemic and
993 central nervous system metabolic alterations in Alzheimer's disease. Alzheimer's
994 Research & Therapy 11:93; doi:10.1186/s13195-019-0551-7.

995 Vardarajan B, Kalia V, Manly J, Brickman A, Reyes-Dumeyer D, Lantigua R, et al. 2020.
996 Differences in plasma metabolites related to Alzheimer's disease, APOE ε4 status, and
997 ethnicity. Alzheimer's & Dementia: Translational Research & Clinical Interventions
998 6:e12025; doi:https://doi.org/10.1002/trc2.12025.

999 Vermeulen R, Schymanski EL, Barabási A-L, Miller GW. 2020. The exposome and health: Where
1000 chemistry meets biology. Science 367:392–396; doi:10.1126/science.aay3164.

1001 Wan Q-L, Fu X, Dai W, Yang J, Luo Z, Meng X, et al. 2020. Uric acid induces stress resistance and
1002 extends the life span through activating the stress response factor DAF-16/FOXO and
1003 SKN-1/NRF2. Aging (Albany NY) 12:2840–2856; doi:10.18632/aging.102781.

1004 Wang C, Saar V, Leung KL, Chen L, Wong G. 2018. Human amyloid β peptide and tau co-
1005 expression impairs behavior and causes specific gene expression changes in
1006 Caenorhabditis elegans. Neurobiol Dis 109:88–101; doi:10.1016/j.nbd.2017.10.003.

1007 Wania F, Mackay D. 1996. Peer reviewed: tracking the distribution of persistent organic
1008 pollutants. Environmental science & technology 30: 390A-396A.

1009 Williams PL, Dusenbery DB. 1988. Using the nematode Caenorhabditis elegans to predict
1010 mammalian acute lethality to metallic salts. Toxicol Ind Health 4:469–478;
1011 doi:10.1177/074823378800400406.

1012 Wytock TP, Zhang M, Jinich A, Fiebig A, Crosson S, Motter AE. 2020. Extreme Antagonism
1013 Arising from Gene-Environment Interactions. Biophysical Journal 119:2074–2086;
1014 doi:10.1016/j.bpj.2020.09.038.

1015 Yan X, Hu Y, Wang B, Wang S, Zhang X. 2020. Metabolic Dysregulation Contributes to the
1016 Progression of Alzheimer's Disease. Front Neurosci 14; doi:10.3389/fnins.2020.530219.

1017 Yu T, Park Y, Johnson JM, Jones DP. 2009. apLCMS—adaptive processing of high-resolution
1018 LC/MS data. Bioinformatics 25:1930–1936; doi:10.1093/bioinformatics/btp291.

1019 Zarse K, Schulz TJ, Birringer M, Ristow M. 2007. Impaired respiration is positively correlated
1020 with decreased life span in Caenorhabditis elegans models of Friedreich Ataxia. The
1021 FASEB Journal 21:1271–1275; doi:https://doi.org/10.1096/fj.06-6994com.

1022

Data sharing

The patient related metabolomics data will be made available on metabolomics workbench. All data and code related to DDT exposure in *C. elegans* is available through a repository on VK's github account https://github.com/vrindakalia/DDT_tau_Celegans.

Tables

Table 1. Demographic data of patients. Patients with a diagnosis of Alzheimer's disease (AD) or mild cognitive impairment (MCI) were included in the analysis. Of these patients, 142 plasma and 78 cerebrospinal fluid (CSF) samples were analyzed using the LC-HRMS method. t-Tau: total tau protein; p-Tau181: tau phosphorylated at threonine 181.

	Control	AD	MCI
PLASMA (N)	46	51	45
% Male	30	35	48
Age (y, mean ± SD)	66.5 ± 8.7	65.9 ± 8.9	69.4 ± 6.6
CSF t-Tau (pg/ml, mean ± SD)	44 ± 23	120 ± 66	76 ± 70
CSF p-Tau181 (pg/ml, mean ± SD)	32 ± 14	74 ± 30	51 ± 25
CSF (N)	25	26	27
% Male	28	38	55
Age (y, mean ± SD)	66.2 ± 8.2	64.8 ± 8.2	70.2 ± 6.2
CSF t-Tau (pg/ml, mean ± SD)	44 ± 24	113 ± 64	69 ± 44
CSF p-Tau181 (pg/ml, mean ± SD)	32 ± 13	79 ± 32	53 ± 20

Figure captions

Figure 1. Global metabolomic features associated with p-tau in humans and *C. elegans*. In A, a metabolome-wide association study found 225 CSF metabolites associated with CSF p-tau levels with $p < 0.05$. Enriched pathways corresponding to CSF p-tau associated metabolites are shown in B. In C, 391 plasma metabolites were found to be associated with CSF p-tau levels, with $p < 0.05$; enriched pathways are listed in D. The aggregating strain shows the greatest influence on the metabolome. In E, a metabolome wide association study found 900 metabolites significantly different between the aggregating and non-aggregating worms. These metabolites resulted in the enriched pathways shown in F. In G and I, Venn diagrams shows the overlap between annotated metabolites associated with p-tau in worms and the human matrix; H and J include the name and KEGG ID for the overlapping metabolites. The nature of the relationship between the metabolite and p-tau, whether positively associated (upward arrow) or negatively associated (downward arrow), is shown under the direction column in H and J.

Figure 2. Uptake and metabolism of DDT and the effect of exposure on growth. In wildtype worms, exposure to increasing levels of DDT shows increasing internal levels of p,p'-DDT and its metabolite, p,p'-DDE while levels of p,p'-DDD were near the limit of detection (A). Wildtype worms exposed to the three doses of DDT were collected in triplicate and the mean level of the parent and its metabolites is plotted with error bars representing the standard deviation. The aggregating strain is smaller in size at larval stage 4 (B, C) and in young adulthood (D, E) compared to the non-aggregating and wildtype strain. Exposure to DDT restricted the growth of all strains at both stages measured. The bars represent the mean measure and the error bars represent the standard deviation. *** Tukey HSD adjusted $p < 0.0001$.

Figure 3. Aggregating tau and DDT affect swimming behavior. The aggregating strain shows altered wave initiation rate (A) and travel speed (B) compared to the wildtype N2 worm. The aggregating strain exposed to DDT spends more time curling while swimming (C). The overall activity index of the aggregating strain is reduced compared to the wildtype N2 strain (D). Each bar represents the mean measure taken from four-five different trials with a total of 50-100 worms per group. The error bars represent the standard error of the mean. * Tukey HSD adjusted $p < 0.05$.

Figure 4. Aggregating tau and DDT inhibits mitochondrial function. In A, a representative oxygen consumption rate (OCR) profile measured using the Seahorse respiratory flux analyzer. The wildtype and non-aggregating strain show a similar OCR however, exposure to DDT reduced the OCR in both strains (A). The aggregating strain shows a reduced OCR compared to the wildtype and non-aggregating strain (A) and exposure to DDT reduced basal respiration in the aggregating strain (B). Each bar represents the mean respiratory measure made across 3-5 experiments with 7-12 wells per run with 3-30 worms per well. The error bar represents the standard deviation. *** Tukey HSD adjusted $p < 0.0001$, * Tukey HSD adjusted $p < 0.05$, ns: not significant.

Figure 5. Metabolomic profile of DDT exposure. In A, a heatmap of the top 25 metabolites with the smallest *p-value* hierarchically clustered shows that in all strains, DDT decreases metabolite intensity. In B, a PCA biplot of PC1 plotted against PC2 shows that strains exposed to DDT cluster differently from the wildtype and non-aggregating control strains. The aggregating strain does not cluster with the wildtype and non-aggregating control groups, suggesting variation as a result of aggregating tau protein expression. In C, levels of uric acid are higher in all worms exposed to DDT and levels of adenosylselenohomocysteine are higher in both: worms exposed to DDT and in worms expressing aggregating tau protein. IMP: inosine monophosphate, FMN: flavin mononucleotide, Ala-Val: alanine-valine dipeptide.

Figure 6. Pathway analysis. The different metabolic pathways enriched in the three different comparison groups. Enrichment is calculated as the ratio of the number of significant hits to the total pathway size.

Figure 7. Associative learning and survival. Associative learning was not affected by exposure to DDT in any of the strains. The aggregating strain did not learn differently from the non-aggregating or wildtype worms. The dotted lines represent the chemotaxis index for each trial with the bold lines representing the mean (A). Each bar represents the learning index (B), calculated as the difference between the trained chemotaxis index, post-conditioning, and the naïve chemotaxis index for each trial (A). The error bars represent the standard error of the mean. The non-aggregating and aggregating strain live shorter than wildtype worms. Exposure to DDT did not affect the survival of the wildtype or non-aggregating strains however, exposure to DDT slightly rescued the reduced lifespan in the aggregating strain. The Kaplan Meier curves (C) are generated by following 60 – 120 worms in each group and the bars (D) represent the mean lifespan in days and the error bars represent the standard deviation. * Tukey HSD adjusted $p < 0.05$.

Figure 1

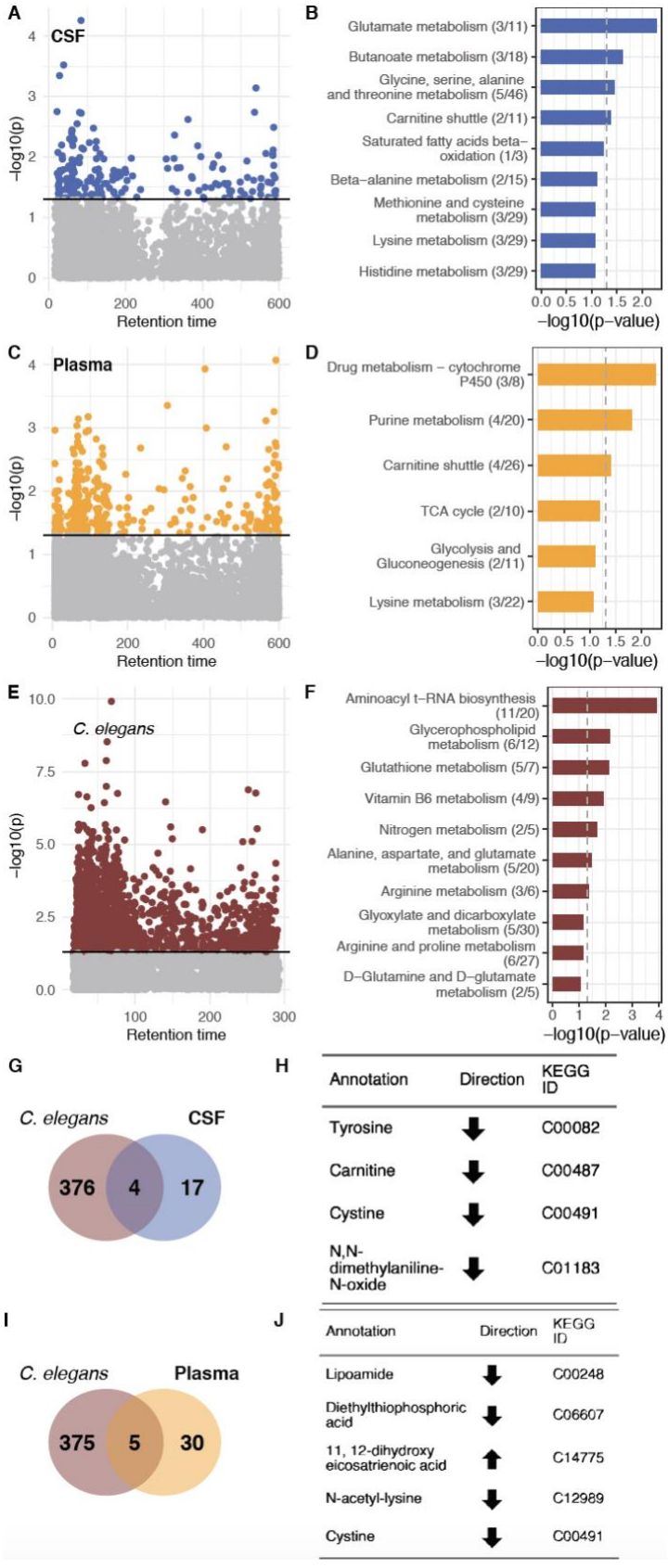

Annotation	Direction	KEGG ID
Tyrosine	↓	C00082
Carnitine	↓	C00487
Cystine	↓	C00491
N,N-dimethylaniline-N-oxide	↓	C01183

Annotation	Direction	KEGG ID
Lipoamide	↓	C00248
Diethylthiophosphoric acid	↓	C06607
11, 12-dihydroxy eicosatrienoic acid	↑	C14775
N-acetyl-lysine	↓	C12989
Cystine	↓	C00491

Figure 2

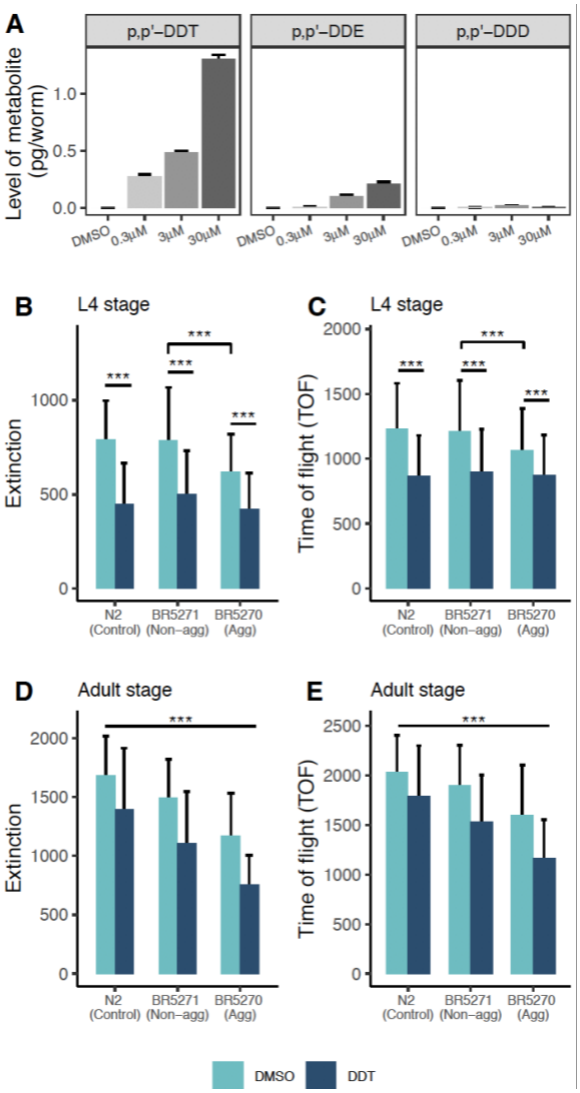

1116 **Figure 3**

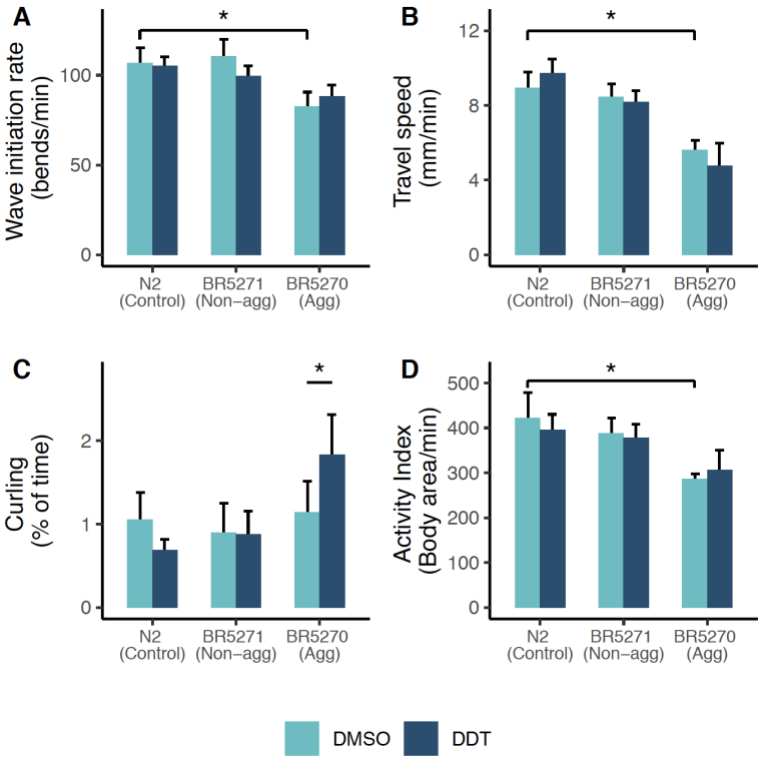

1117

1118

1119 **Figure 4**

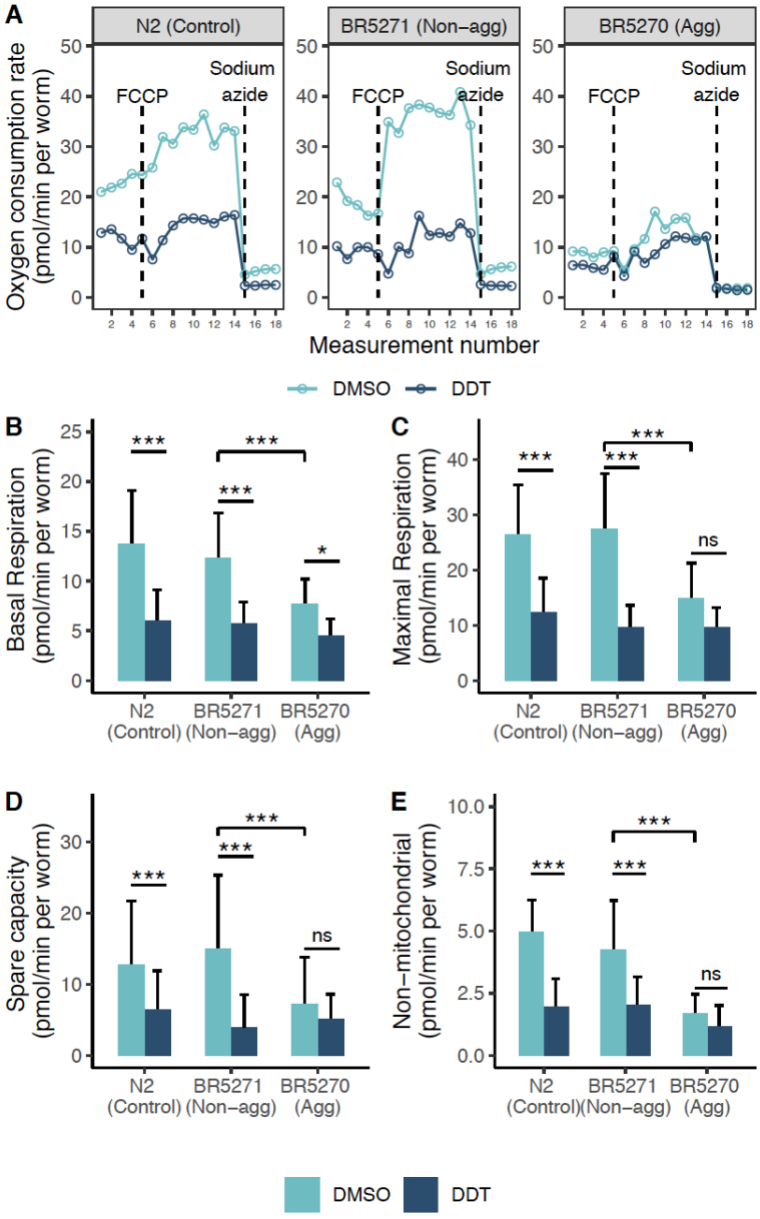

1120

1121

1122 **Figure 5**

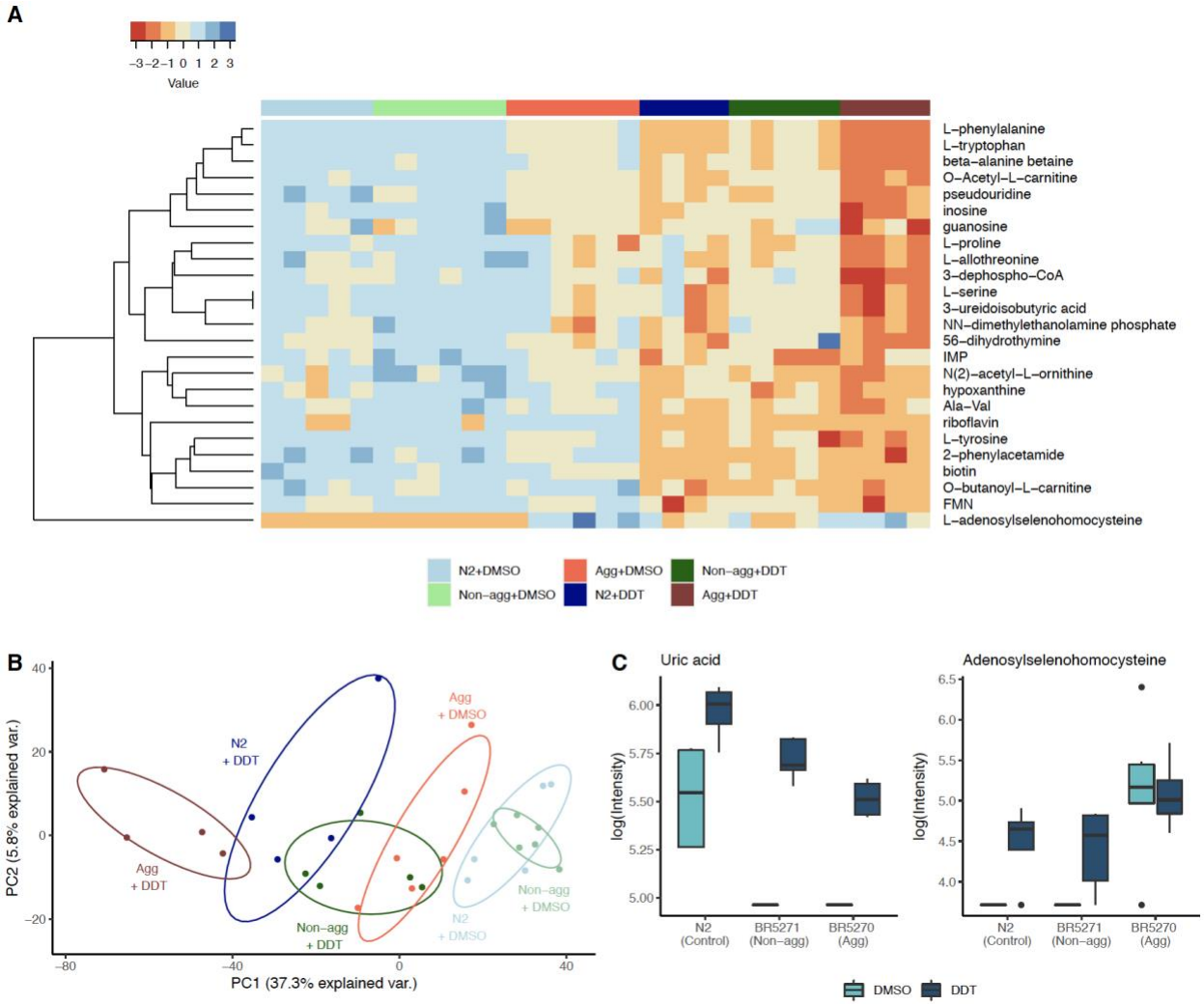

1123

1124

1125 **Figure 6**

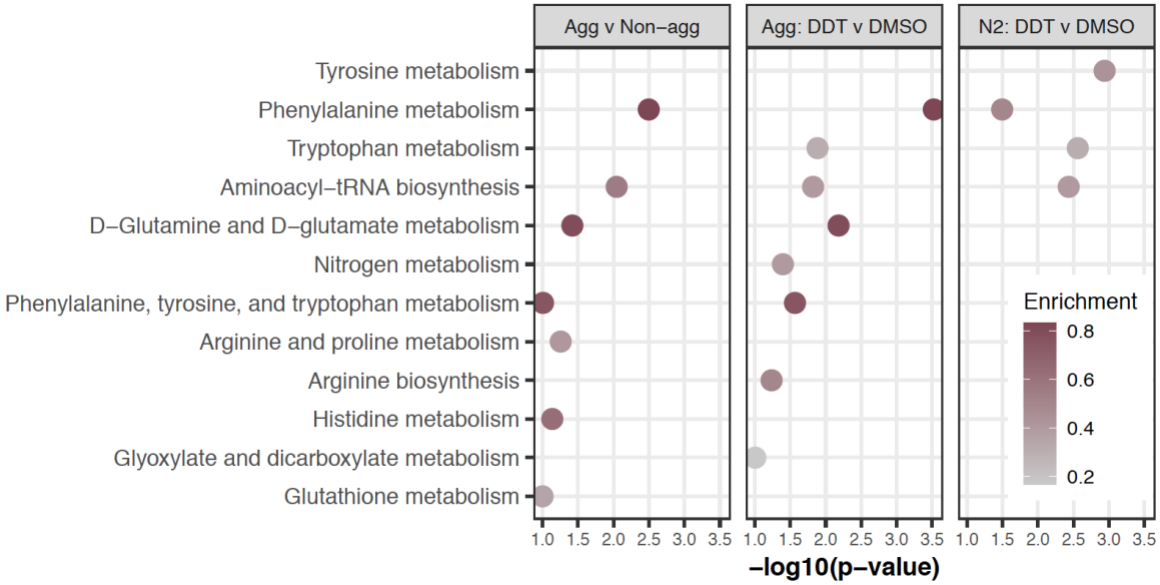

1126

1127

1128 **Figure 7**

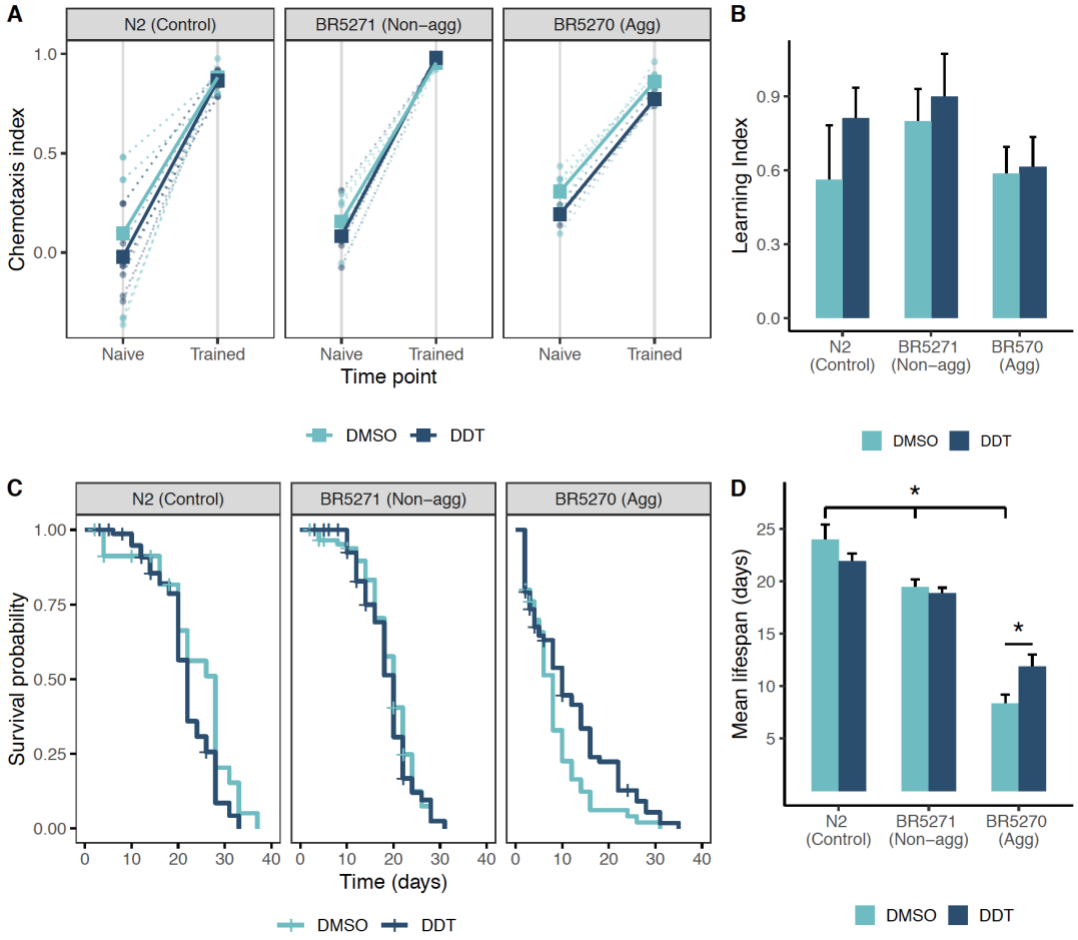

1129

1130

1131